Title
MRI-guided endovascular intervention: current methods and future potential.

Journal
Expert Review of Medical Devices, 19(10)

Authors
Kilbride, Bridget
Jordan, Caroline
Mueller, Kerstin
et al.

Publication Date
2022-10-01

DOI
10.1080/17434440.2022.2141110

Peer reviewed

HHS Public Access

Author manuscript

Expert Rev Med Devices. Author manuscript; available in PMC 2023 October 01.

Published in final edited form as:

Expert Rev Med Devices. 2022 October ; 19(10): 763–778. doi:10.1080/17434440.2022.2141110.

MRI-guided endovascular intervention: current methods and future potential

Bridget F. Kilbride[1], **Kazim H. Narsinh**[1], **Caroline D. Jordan**[2], **Kerstin Mueller**[3], **Teri Moore**[1], **Alastair J. Martin**[1], **Mark W. Wilson**[1], **Steven W. Hetts**[1,*]

[1]Department of Radiology and Biomedical Imaging, University of California, San Francisco, San Francisco, CA, USA

[2]EnMed, Texas A&M University, Houston, TX, USA

[3]Siemens Medical Solutions USA Inc., Malvern, PA, USA

Abstract

Introduction: Image-guided endovascular interventions, performed using the insertion and navigation of catheters through the vasculature, have been increasing in number over the years, as minimally invasive procedures continue to replace invasive surgical procedures. Such endovascular interventions are almost exclusively performed under x-ray fluoroscopy, which has the best spatial and temporal resolution of all clinical imaging modalities. Magnetic resonance imaging (MRI) offers unique advantages and could be an attractive alternative to conventional x-ray guidance, but also brings with it distinctive challenges.

Areas covered: In this review, the benefits and limitations of MRI-guided endovascular interventions are addressed, systems and devices for guiding such interventions are summarized, and clinical applications are discussed.

Expert opinion: MRI-guided endovascular interventions are still relatively new to the interventional radiology field, since significant technical hurdles remain to justify significant costs and demonstrate safety, design, and robustness. Clinical applications of MRI-guided interventions are promising but their full potential may not be realized until proper tools designed to function in the MRI environment are available. Translational research and further preclinical studies are needed before MRI-guided interventions will be practical in a clinical interventional setting.

[*]***Corresponding Author:*** Steven W. Hetts, steven.hetts@ucsf.edu, Department of Radiology and Biomedical Imaging, University of California San Francisco, 185 Berry Street, Suite 350, San Francisco, CA 94107.

Declaration of interest

Steven W. Hetts declares Grant support from NIH paid to UCSF; Research contracts from Siemens Medical Solutions, Route 92 Medical, and Stryker Neurovascular paid to UCSF; Payments from Data Safety and Monitoring Committee for Imperative Care, Cerenovus, and MicroVention Terumo; Equity in ThrombX and Filtro, Inc. None of these are directly relevant to the work presented. Kerstin Mueller is an Employee of Siemens Medical Solutions USA Inc. Alastair J. Martin has received a research grant support from ClearPoint Neuro and is a consultant for Iota Biosciences. The authors have no other relevant affiliations or financial involvement with any organization or entity with a financial interest in or financial conflict with the subject matter or materials discussed in the manuscript apart from those disclosed.

Reviewers Disclosure

One of the reviewers has several investments in companies that produce iMRI components and own patents in that field. The other peer reviewers on this manuscript have no relevant financial relationships or otherwise to disclose.

Keywords

MRI-guided; endovascular intervention; interventional radiology; interventional MRI; minimally invasive surgery; robot-assisted; MRI safety; real-time MRI

1.0 Introduction

The main therapy for many vascular diseases, along with drug treatment, is image-guided endovascular intervention. Endovascular interventions are typically performed by inserting a catheter into the femoral artery, which is then navigated under x-ray guidance through the vasculature to the treatment site. The diseased area may be a portion of the vessel wall that has weakened to form an aneurysm susceptible to hemorrhage, or a vessel may become stenotic or occluded by a plaque or clot. Vessels can also become sites of abnormal growth in the case of vascular malformation. The endovascular intervention may involve catheter-based delivery of an embolic material or therapy drug, or deployment of a medical device, such as a detachable aneurysm coil or stent to allow blood flow through a stenotic vessel. Furthermore, another important treatment application lies in oncology, in which chemotherapy drugs or radiation-emitting particles can be delivered directly to the vascular bed feeding a tumor. Minimally invasive procedures, such as endovascular intervention, continue to replace invasive surgical procedures because of their effectiveness with reduced mortality, morbidity, and strain on hospital resources [1].

Most endovascular interventions today are guided by x-ray fluoroscopy because of its temporal and spatial resolution [2,3], utilizing flexible catheters with optimized mechanical properties. The concept of utilizing magnetic resonance imaging (MRI) in interventional procedures began in the late 1980s, where the focus was on MR-guided biopsies [4–6]. In parallel with this innovative work, plastics for catheters and stents were beginning to be identified to expand the arsenal of MR-compatible and visible materials [7,8], and interest in endovascular interventions began to increase [9,10]. Since then, the field of interventional radiology has adopted various new technologies in MR imaging and medical devices to improve treatment efficacy of image-guided endovascular interventions. MRI offers unique advantages for image guidance, but also brings with it different challenges. MRI provides superior soft-tissue contrast, has no ionizing radiation, and allows for measurement of quantitative biomarkers, making it an attractive alternative to x-ray [11,12]. However, several challenges have limited the widespread adoption of interventional MRI, including lack of fast, real-time imaging, scanner utilization, device visualization, MRI safety, and interventionalist ergonomics.

In this paper, we discuss the basic features and current status of MRI-guided endovascular interventions in terms of the MR imaging system, interventional equipment and devices, procedure characteristics, and personnel involved. We will first give an overview of the current state of MRI-guided endovascular interventions, and then speculate on future potential about each category, providing the rationale and evidence for each prediction.

2.0 MRI system

2.1 Magnet and suite configurations

Early low-field MRI systems became available in various formats to facilitate patient access during intervention. The first dedicated interventional MRI, the Toshiba ACCESS, was a 0.064T open system with 360° horizonal “temple” access [13]. Other early designs included C-arm shaped 0.2T Siemens Magnetom OPEN and 0.23T Picker Outlook [14] and additional open systems like the 0.3T Hitachi Airis. These initial systems provided significant horizontal access, but full patient access was suboptimal [15]. The GE Signa 0.5T “double donut”, was then conceived to allow flexible vertical and horizontal patient access through a vertical gap between two superconducting rings [16].

In other approaches, conventional systems have been adapted for intraoperative scanning. Careful attention must be paid to the integration of surgical and MR environments, requiring a multidisciplinary approach among groups including relevant medical specialties, hospital engineers and physicists, and facilities planning, to name a few[17]. The University of Minnesota Intraoperative MRI suite with Philips employed a mobile operating table, permitting rotation outside the 5-gauss line for neurosurgical operation with MRI-compatible tools and into the magnet for imaging [18]. The 1.5T Philips Gyroscan ACS-NT also featured 100-cm tapers on the front and rear, enhancing patient access with two potential surgical areas. Additionally, the Siemens Brain Suite, in collaboration with Brain LAB, implemented a similar rotating operating table in conjunction with a conventional 1.5T scanner [19,20].

The aforementioned MRI scanner configurations have seen suboptimal utilization because of their location in a sterile environment and the lack of MRI scanning being performed during operation. As a result, a clear need has surfaced to perform diagnostic MRI scans independently of lengthy operations. Concepts of movable scanners in dual-, or multi-room, designs have been presented to maximize operational usability of scanners for both diagnostic and surgical purposes in this way. First reports using a single-room movable 1.5T MRI system [21,22], and later dual-room solutions with a movable magnet have been proposed [23]. In these formats, the scanner can move into an operating room, either or via ceiling rails (IMRIS, Winnipeg, Canada), or as a mobile unit [24,25]. Various multi-room arrangements exist with multimodality imaging capabilities at the present. At Yale University, there is a hybrid IMRIS system with a ceiling-rail mounted 3.0T MRI scanner and biplane angiography system. The interventional cardiac MRI suite at the NIH has a 1.5T Siemens Sonata scanner, including a screen, shielded projector, and headphones. A Siemens Axiom Artis FC single-plane angiography system is in an adjacent room, where there is anesthesia equipment, lights, large displays, and an injector [26]. The two imaging suites are separated by RF-shielded doors to permit independent use of each system or simultaneous use with a motorized transfer table. At Brigham and Women’s Hospital (BWH) and Harvard Medical School, the Advanced Multimodality Image-Guided Operating (AMIGO) suite has three connecting rooms that include an interventional PET/CT scanner, an x-ray fluoroscopy table and C-arm, and a 3.0T MRI scanner (Figure 1A) [27]. At University of California, San Francisco’s affiliated Zuckerberg San Francisco General Hospital, there is a fully integrated

two-room x-ray angiography and MRI (AMR) suite (Figure 1B). The AMR suite is equipped with a full-featured Siemens Artis Q biplane angiographic system and a full diagnostic Siemens Magnetom Skyra 3.0T MRI scanner [28]. These multimodality interventional imaging suites function as test beds for advanced interventions, enabling independent use of the best features of each type of imaging during different phases of an operation.

2.2 Ancillary accessories

A standard x-ray angiography suite typically includes a number of equipment units, multiple operators, imaging control, image display, easy communication in a quiet room with patient and staff, nurses, anesthesiologists, and devices. Standard equipment used in angiography suites often are not compatible for use in the MRI suite, such as anesthesia pumps and ventilators, and oxygen tanks. While there are commercially available MRI-conditional versions, user interfaces may vary, underscoring the need for proper training and in-servicing of MRI-conditional equipment prior to use. The staff needs to be comfortable with and trained on the different interfaces and functionality of the MRI-safe and compatible equipment. MRI-conditional equipment must be clearly marked to ensure that incompatible, potentially dangerous equipment is not introduced to the MRI environment.

For real-time navigation, in-room LCD displays have been developed by Cambridge Research Systems and NordicNeuroLabs to be compatible with 1.5, 3.0, and 7.0T environments outside the Gaussian lines. Communication within the MRI suite between the patients, in-room staff, and control room staff must also be taken into consideration. Standard MRI sequences are loud and require personnel to wear headphones during scans. One solution is noise-cancelling wireless headsets with multiple transceivers around the suite using diffuse infrared technology, with multiple channels to allow movement and communication (IMROC IR™ Wireless Communication, OptoAcoustics, Tel Aviv, Israel). These headphones would be of particular use when the patient is under conscious sedation, where communication with staff is critical. MRI vendors also now offer quiet imaging modes, which may be applicable to the interventional setting provided the imaging requirements are not compromised in a substantive way.

2.3 Real-time imaging and guidance

Diagnostic MRI has off-line reconstruction and fixed scan protocols. For real-time imaging, reconstruction must be done within a few hundred milliseconds, inline reconstruction with low latency. The introduction of the sliding window technique was essential in allowing MRI to reach real-time frame rates, allowing for the beginning of “MR fluoroscopy” [29]. The sliding window approach initially collects an image with full k-space coverage. The acquisition continues and previously acquired k-space lines are replaced with the most current data. Thus, images can be acquired more rapidly than the time it takes to acquire the full k-space data. The image update rate is then defined by the window of new data that is acquired before an image update is obtained. With this approach an image display rate of 12.5 images/second was achieved with a single coil. This first work resulted in image acquisition time of 250–1000 ms, imaging rate as high as 30 Hz, and a reconstruction time of 67ms [29]. This could be sped up by upwards of 8 times if the approach is parallelized, in combination with larger coil arrays [30,31].

One major challenge in the interventional MRI suite is that personnel and image displays need to be inside the scan room, compared to diagnostic imaging, where there are fixed protocols, image review is done off-line, and no personnel are in the scan room. During an endovascular intervention, the interventionalist needs interactive scan control patient-side, real-time acquisition and reconstruction, possibly hemodynamic recording for cardiac applications, and ability to scan devices. MRI safety training is imperative. Part of the interactive scan control requires being able to change parameters. For the real-time display interfaces, the MRI system vendor's have their own platforms, and several third-party platforms have been developed, including HeartVista's research platform, RTHawk [32], OpenIGTLink [33], and VURTIGO [34]. Recently, one research group developed a real-time acquisition and reconstruction system using mixed-reality 3D display for cardiac MRI-guided procedures [35], demonstrating that mixed-reality could potentially be used for real-time intervention in the future.

2.4 Robotic assistance systems

Within typical high-field, closed-bore MRI scanners, patient access is limited, presenting uncomfortable and unergonomic conditions. Robotic-assisted systems have been developed to address the issue of patient access without sacrificing physician ergonomics or image quality. In fact, robotic systems have been realized to function in the MRI environment for multiple surgical applications, yet dedicated systems for minimally invasive procedures are less common and have yet to find market success. This could be partially due to the material limitations presented by MRI, as metallic, ferromagnetic materials must be avoided to maintain sufficient image quality and MRI-conditional status. The field of MRI-guided robotic interventions continues to see innovation with many benefits including improved precision and stability, less interventional trauma, and shortened patient recovery times [36].

Robotic systems designed to augment MRI-guided needle placement is an active area of research, but none have yet to become commercially available. For example, the GantryMate (Interventional Systems, Kitzbühel, Austria) is an MR-compatible system constructed from plastic and fiberglass materials and Bowden cables are used to translate mechanical manipulation [37]. More sophisticated roboticized systems with various actuators are used to remotely manipulate working arms from the control room. The ArthroBot is a remote-controlled, body-mounted robot operating with 4 degrees of freedom (DoF) for MRI-guided needle placement during shoulder arthrography [38]. Similarly, the PainBot features the same 4 DoF system, with an added 2 DoF needle driver system to provide rotation and translation from a driver box for perineural injections. As presented by Cleary, et al., an MRI-safe robot was developed with 3 DoF for pediatric long bone biopsy, using pneumatic actuation and MRI-safe construction materials [39]. Furthermore, the robot controller is in the control room, and data encoding is entirely light or optical, presenting virtually no interference.

While there are commercially available patient-and-control room-side operated systems for endovascular interventions under x-ray guidance, such as the CorPath GRX platform (Corindus, a Siemens Healthineers Company, Watham, MA, USA), equivalent systems for MRI are not yet available. Kundrat, et al., have designed a novel MRI-safe robot for

master-slave remote manipulation of guidewires and catheters [40], which may pave the way for future MRI-guided interventions. The robot operates with valve-based pneumatic actuation in 6 DoF, and the physician may easily switch the driver mode between the catheter and guidewire. The slave robot and pneumatic tubing are single-use disposable products, eliminating the need for sterilization between procedures.

3.0 Devices for MRI-guided procedures

3.1 Safety considerations

Fundamental design of interventional devices is important to understand for safe translation into interventional MRI procedures. Typical guidewires and catheters used for guiding interventions under x-ray fluoroscopy feature metallic components in their construction. In the case of guidewires, there is usually the core wire, tip, body, and coating material [41], with the core wire contributing most of the mechanical characteristics. On the other hand, catheters primarily utilize a reinforcement layer that is coiled, braided, or a combination of the two, sealed between a lubricious inner liner and a thermoplastic outer jacket. Like the core wire of a guidewire, the reinforcement layer of a catheter confers most of the device's mechanical characteristics.

In both guidewire cores and catheter reinforcement, metallic alloys are employed on a device basis for optimized mechanics such as controlled flexibility, pushability, torque response, and kink resistance. They can be stainless steel and nitinol (Nickel-Titanium) alloys in the case of guidewire cores, and catheters braids may also use 304 V, 304 L, and 316 L stainless steels or tungsten [41]. However, due to multiple risk factors in the unique working environment of MR suites, metal components in interventional devices are greatly limited. Stainless steel may not be compatible with MRI scans, as it has variable metal composition and can be ferromagnetic, introducing risk of force and torque from the static magnetic B_0 field. Nitinol, a widely used shape memory alloy, is not ferromagnetic, thus not susceptible to magnetic-induced torque or displacement. These metals function as long conductive structures in braids and wires, interacting with the RF pulses and coupling with the electric field of the transmit RF coil, resulting in elevated power deposition and local specific absorption rate (SAR) at the device tip [42,43]. A major safety hazard arises from this coupling with the transmit RF field, as tissue immediately adjacent to the device tip can undergo unsafe heating during a scan. In one classic paper, a Terumo standard angiography guidewire, consisting of nitinol, was partially immersed in a saline bath to simulate an endovascular intervention. During a gradient echo (GRE) sequence with an average SAR of 3.9W/kg at 1.5T, the distal tip increased from room temperature at 26°C to 74°C after only 30 seconds of scanning [44], demonstrating the danger from not only the heating, but also the very short amount of time required to reach that temperature.

It has been found that conductive components longer than a quarter wavelength at resonant frequency are subject to standing wave formation and RF-heating. Yeung et al. determined that significant SAR gain occurred when the length of a conductive component was longer than a quarter wavelength at resonant frequency, which was approximately 12 cm in humans at 1.5T[45]. By maintaining component lengths shorter than a quarter wavelength, standing wave formation can be avoided and RF-induced heating is mitigated. Multiple groups

have identified additional manufacturing steps to achieve MR-compatibility when using metal components. For example, Basar, et al., used a segmented nitinol guidewire for use at 1.5T with connectors of similar mechanical performance in the gaps to eliminate intermittent areas of mechanical weakness [46]. Adapting a similar approach with laser segmentation, Yildirim et al. demonstrated catheters for MRI-guided cardiac interventions through segmentation of a nitinol braid to mitigate device heating without significantly compromising mechanical properties at 1.5T [47]. These manufacturing techniques appear to preserve mechanical performance without the cost of unsafe device heating, but comprehensive mechanical characterization, as required for regulatory approval, has yet to be performed. More importantly, segmentation parameters much be refined and adjusted on a scanner basis, as non-resonant segment lengths would shorten at higher field strengths.

While polymers may not possess ideal elasticity, there may still exist alternatives to metallic reinforcement that have sufficient mechanical performance in specific use cases. Like metallic materials, shape memory polymers utilize high glass transition temperatures to permit heat setting of various desired tip shapes. In another approach, polymers can be strategically selected such that their recovery glass transition temperature is at body temperature (37°C) [48]. These properties allow for devices to be introduced with high stiffness while softening during navigation within the body. Promising polymer candidates have been identified such as para-aramids, liquid crystal polymer, and poly(ether) ether ketone [49,50]. As with the introduction of new manufacturing methods, full mechanical characterization is necessary to support regulatory approval. For interventional devices, common failure modes resulting from insufficient reinforcement include severe bending and kinking, fracturing, separation, and insufficient torque response. In order to obtain regulatory approval, catheters and guidewires must be thoroughly characterized per ISO 10555–1:2013 and ISO 11070:2014, respectively [51,52]

Advances in device engineering have made great strides in driving interventional MRI procedures closer to clinical practice, with preliminary studies completed in swine [53–55]. Before this, device safety bench tests including force and torque from the main static B_0 field and RF-induced heating from the B_1 field should be performed. At a minimum, devices must meet the ASTM standards for MRI-conditional status, which may require phantom testing and simulations [56–58]. Second, for devices to be used clinically, they must also comply with ASTM and ISO standards for sterility and durability. After further development, the next step will be to perform in-human clinical trials and demonstrate non-inferiority when compared to conventional x-ray fluoroscopy devices.

Safety protocols have been established for interventional MRI procedures [59], but they must be revisited with the introduction of new technology. Training is essential to incorporate proper safety checks into the workflow of the surrounding area and the MRI suite. Personnel entering the MRI suite should be checked for metallic materials. Prior to entering the MRI suite, the patient must be checked for potentially dangerous metallic materials, such as EKG electrodes or pacemakers. Equipment entering the MRI suite, such as anesthesia pumps, ventilators, and gas tanks, must be at least MRI-conditional and clearly marked as such in accordance with ASTM standards [60,61]. If equipment is not safe to

enter the MRI suite, tubing and wires may be routed through RF-shielded wall conduits to the patient, introducing additional layers of complexity to interventional MRI procedures.

3.2 Guidewires

Two companies have designed guidewires that use a fiber-reinforced material instead of metal braiding for enhanced MRI safety and visualization. The first-in-man intervention was performed using a nitinol-tipped guidewire with iron-doped fiberglass passive markers for patients with valvar pulmonary stenosis [62]. MaRVis Interventional GmbH has obtained CE Mark for their guidewire, MaRVis Amber Wire, which comes in several different diameters, types, tips, and lengths [63]. It is constructed of glass or aramid fibers impregnated by epoxy resin, with a core rod containing iron oxide nanoparticles to induce susceptibility artifacts down the length of the shaft [53,64]. Nano4imaging has a guidewire with MRI conditional status, the MRWire EmeryGlide™, with CE mark and FDA 510K approval for use at 1.5T and 3.0T. It also contains discrete markers, and the length of the wire is radiopaque [65]. While one approach might be to modify the reinforcement materials of a guidewire, there are a number of previously proposed solutions to mitigate RF-induced heating, including various RF transmit solutions [66–68], device modification [69–72], and sequence modification/power limits [73,74]. One relevant example of sequence modification and power limits was recently demonstrated, where the investigators were able to limit the heating of a specific fully insulated metallic nitinol guidewire (150 cm, 0.035” Terumo *Glidewire*) to an increase of just 0.07°C, using a low-SAR imaging sequence at 1.5T [75]. The imaging protocol used a reduced flip angle (10°) GRE acquisition, with a longer repetition time (TR) spiral readout (10ms) for cardiac MR (CMR) fluoroscopy. The authors emphasized that this needs to be verified for each scanner, as certain parameters may change between different vendors. At lower field strengths (i.e. 0.55T), RF heating of guidewires becomes less of a concern, at the tradeoff of reduced SNR and lower polarization [76]. Lastly, parallel transmit (PTx) coil arrays have recently demonstrated safe visualization of unmodified guidewires [77]. In this study, current sensors were placed over a standard guidewire to determine RF-induced current modes during interventional CMR. The PTx system uses maximum and null current modes to safely image with a guidewire *in situ*; however, this approach has noticeable signal drop-off at the distal tip.

3.3 Catheters and MRI-visible markers

MRI visualization markers for catheters or guidewires are typically categorized as passive, active, or resonant (also referred to as semi-active) [78]. Passive approaches use differences in magnetic susceptibility between the device and surroundings, such as gadolinium or iron oxide particles, to cause local B_0 field inhomogeneities, giving rise to signal voids [79,80,9,81]. Their visibility may suffer from partial volume artifacts and diminished contrast in the image. One of the first implementations was real-time MR fluoroscopy of an MRI-guided iliac artery stent placement using dysprosium (Dy) doped catheters (Figure 2) [82]. An early preclinical application of a passively-tracked catheter used a gadolinium (Gd) filled balloon for iliac artery stenosis in animal models [83]. Another example was a CO_2-filled balloon for cardiac catheterization in patients to measure pressure [84]. These devices were then able to demonstrate feasibility of pulmonary vascular resistance using pressure measurements combined with blood flow measurements [85], demonstrating

improved accuracy than the gold standard. This was further extended in a larger patient study, allowing accurate stratification for intervention in patients with congenital heart disease [86]. MRI-guided diagnostic cardiac catheterization is now regularly performed in patients at the NIH using passive air or gadolinium-filled catheters [87].

Active markers, such as micro receive coils, may supply a direct current (DC) to a coil on the catheter [88–90], or in another approach, may use miniature transmit-receive coils [91]. Active tracking has been achieved with MRI needles featuring an elongated loop coil and multiple tight windings with passive guidewires [92], and more recently, a single-loop coil with multiple solenoid coils printed in conductive ink down the shaft of a nitinol-based needle [93]. First in-human feasibility studies of actively tracked catheters were demonstrated with interactive software (iSuite, Philips Healthcare, Best, Netherlands) to display an electrogram measuring the isochrone for an electrophysiology procedure to ablate an atrial arrhythmia [94,95]. This work has been built upon to develop a portfolio of MRI-conditional steerable diagnostic and ablation catheters (Imricor, Minneapolis, MN, USA), which recently received their CE marks. Active tracking is challenged by the requirement to supply external current via conductive wires down the length of the catheter, which are susceptible to local RF-induced heating at the device tip [44]. Moreover, transmission lines occupy precious space in the small working channel, making manufacturing of interventional devices with decreasing diameters a considerable challenge. Studies have sought to mitigate heating by utilizing high-resistivity coaxial cable [96] and modifications such as coaxial chokes to reduce undesirable currents. Recent work has used acousto-optic markers, using optical fibers for signal transmission at 0.55T [97]. There is still room for improvement to adapt these techniques to higher field strength scanners and smaller devices.

Wireless resonant circuit markers, or inductively coupled RF coils, can be implemented as a circuit with a capacitor (C) connected to a coil, which has inductance (L) and intrinsic resistance (R). This RLC circuit can be built on the distal tip of the catheter to provide local signal amplification of the B_{1+} field [98,99]. The circuit inductively couples with the RF transmit coil, inducing current, which is then amplified through the resonant circuit. This causes the local RF field to increase, resulting in local signal amplification and a localized bright signal at low input RF levels. Such wireless resonant circuits [100], also known as inductively coupled RF coils [101], have previously been built on top of large diameter guide catheters using a variety of fabrication methods and geometries. These wireless circuits eliminate the need for wires running down the length of the catheter for visualization, ultimately reducing heating risks that plague active tracking methods. Wireless resonant circuits have been built more recently on catheters for interventional MRI, using inductor coil geometries including rectangular surface loop coil [102], two opposing solenoids oriented at 45° relative to the major axis of the catheter [103], and flat spiral coils [104]. Recent work proposed a hand-wound circuit with an inductor geometry of a double helix, with each arm tilted 45° with respect to the z-axis [105,106], which was then 3D-printed, with feasibility shown *in vitro* and *in vivo* [107] (Figure 3). As with active tracking, resonant approaches may suffer from bulky components, leading to large device size and suboptimal device rigidity. As a result, a number of other microfabrication methods for building markers on catheters have been explored beyond manual wire winding, including flexible printed circuit boards, hot embossing, thin-film techniques, and aerosol

deposition processes [108]. One group designed and manufactured rectangular spiral planar coils stacked in multiple layers, with a size of $6.7\times1.5\times0.3$ mm^3, built on flexible printed circuit boards, and incorporated it onto needles and catheters [109]. The aforementioned techniques remain in investigative phases of feasibility and material property exploration with limited *in vivo* data.

3.4 Steerable/direct current catheters

Visualization is one important aspect for navigation, and other forms of navigation assistance have manifested in steerable catheters. These devices offer the ability to torque the distal tip through some of the most tortuous anatomy [110]. Manual actuation was demonstrated by Clogenson et al., where the distal tip of a multi-selective catheter was actuated via pull-wires [111]. Gosselin et al. exploited the gradient forces during MRI scanning to steer a catheter tipped with ferromagnetic spheres [112]. These spheres ultimately could cause unintended displacement, arising from dipole-dipole interactions. Other potential limitations that could make navigation difficult include image artifacts induced by the spheres and the physical weight of the tip causing traumatic shear stress on vessel walls [113].

Steering can also be achieved via remote controlled catheters actuated by applying direct current to coils at the distal tip. An induced magnetic field at the catheter tip then interacts with the static field of an MRI scanner, allowing on-demand application of field-aligning torque. Lillaney et al. demonstrated renal embolization in a swine model at 1.5T [114]. As with active tracking methods, long wires supply current to the steering coils, which were susceptible to heating and melting of insulative jacket materials. Later work determined safe upper current limits to avoid such heating [115]. Liu et al. modeled a magnetically-actuated steerable catheter in three-dimensional space [116], and improved upon it using open-loop control [117], building on prior work from Guidino et al. with an array of active steering coils [118]. Early iterations of steering coils may lack the low profiles needed for endovascular intervention, resulting in rigid and cumbersome devices that are unnavigable (i.e. do not “track”) in finer vasculature, making advanced manufacturing methods (i.e. laser lithography) important for low-profile technology.

3.5 Tracking sequences

Active tracking is achieved with tracking sequences that use intermittent non-selective excitations combined with spatially encoding gradients [119]. The first MRI tracking sequence of an active marker, a micro-coil, used four projections to acquire the coil position [88]. Next, continuous radial MRI was introduced for real-time simultaneous acquisition of anatomical MRI and tracking of micro-coils [120]. With additional distributed memory capability, any arbitrary *k*-space trajectory was then possible to use for real-time MRI [121]. Then, bSSFP sequences were implemented real-time [122]. Later, Hadamard encoding and phase dithering were added to improve the active catheter tracking sequence [91]. This was further implemented for use in tracking wireless resonant circuits [100]. Another real-time active tracking method added a tracking block to a bSSFP and spoiled gradient recalled echo (GRE) sequence, and repeated the block four times with different readout gradient polarities to correct for off-resonance [123].

Several groups have developed real-time or near real-time MRI sequences for use in conjunction with a passive tracking strategy. Bakker et al. proposed contrast-enhanced MR fluoroscopy as a tracking method in conjunction with passive catheters and guidewires [9]. Martin et al. developed a digital subtraction MR angiography roadmap to track steerable catheters with passive contrast [124]. Another method tracked a catheter with a passive ferromagnetic tip using dual-echo projections [125], by using off-resonant excitation and rephasing gradient to selectively excite and conserve the signal around a sphere. To remove the background signal and preserve the signal in the selected region, two projections are acquired in one echo train with orthogonal direction of the rephasing gradients. There have also been developments of new visualization methods in combination with tracking, such as white marker imaging, which make the passive signal dropout of a passive marker turn bright (Figure 4) [126]. Patil et al. developed automatic slice positioning for passive real-time tracking of devices [81], by using their susceptibility shape and dephasing gradients interleaved in sequence. Concurrent contrasted-enhanced visualization of patient anatomy and gadolinium-filled balloon catheters has been achieved by Forte et al. through partial saturation (pSAT) sequences comprised of a single shot acquisition with bSSFP readout preceded by a partial saturation pre-pulse [127]. Overall, passive tracking often requires specific pulse sequence modifications tracking to avoid partial volume effects by imaging across thicker slices, but contrast to noise may be sacrificed in the process.

4.0 Clinical applications

4.1 Cardiovascular applications

Promising cardiovascular applications include not only identification and treatment of coronary atherosclerosis but also evaluation and treatment of congenital heart disease and electrophysiology [119,128–130]. Razavi et al. performed MRI-guided cardiac catheterization in sixteen patients with congenital heart disease for purposes of diagnosis and evaluation, including two radiofrequency ablations [84]. The elimination of ionizing radiation was particularly meaningful in these cases, since they were performed on children and teenagers [84]. Performing these procedures under MRI has the added benefit of permitting any slice orientation. Recently, Campbell-Washburn et al. performed right heart catheterization using a metallic guidewire, and using a low SAR sequence, measured negligible heating (<0.07°C) using a standard angled-tip nitinol Terumo Glidewire [75]. Ratnayaka et al. performed 50 cardiac MR fluoroscopy guided right heart catheterizations in 39 pediatric patients, using passive catheters [131].

In the pilot studies outlined above, the standard fluoroscopic procedure was largely copied directly to MRI to demonstrate feasibility; however, they have yet to show a clear advantage of real-time MRI guidance beyond the avoidance of exposure to ionizing radiation. Further modifications will be needed before any endovascular MRI-guided procedure can be adopted for more widespread clinical use.

In the future, more difficult cardiac procedures, such as treatment of ventricular tachycardia could benefit from MRI-guided procedures. Another compelling MRI application is measuring force, as well as ablation area and temperature, and correlating with the late gadolinium enhanced images (trans-septal puncture) [129,132,133]. Real-time MR

thermometry has also been used to quantitate thermal dose during real-time ablation, which was recently demonstrated and implemented in Gadgetron: An open-source framework for medical image reconstruction [134]. Moreover, Gadgetron has been shown as a platform for high-resolution spiral imaging to image guidewires navigating into the heart [135,136].

4.2 Peripheral arterial applications

MRI guidance to perform endovascular procedures offers the possibility to quantitatively measure success in real-time while performing the procedure without having to move the patient. Procedures that could benefit from intra-procedural imaging of a physiologic biomarker and superior soft tissue contrast are of particular interest. For example, pelvic, femoral, and popliteal artery stenosis have been stented using real-time endovascular MRI [137,138]. Manke et al. demonstrated feasibility of performing angioplasty and placing stents in thirteen patients with iliac stenosis [137]. Overall, while the procedure was feasible, it was limited by lack of real-time monitoring, stent artifacts and long procedure times [137]. Similarly, Paetzel et al. demonstrated real-time MR-guided balloon angioplasty of femoral and popliteal stenoses [139]. Their research benefitted by lack of stent use (limiting image-based artifact), injection of gadolinium into the angioplasty balloon for visualization, and pre and post intra-arterial MR angiography [138]. This research shows promise, particularly with current advancements in MR imaging techniques, highlighted by the use of MRI to evaluate intra-plaque hemorrhage in high-risk atherosclerotic plaque and quantitate flow [140]. Non-invasive MRI assessment of arterial plaque morphology could help guide intervention in the future [128,140].

4.3 Oncology applications

4.3.1 Central nervous system oncology—MRI has been adopted over other modalities for diagnosis and management of multiple oncologic diseases because of superior soft tissue contrast and the ability to obtain multiparametric tissue characterization. Recent research has found value in MRI during osmotic blood-brain barrier opening (OBBBO) to increase treatment efficacy of intra-arterial therapies for primary and metastatic disease in the brain. The current gold standard for such procedures is x-ray digital subtraction angiography (DSA), though it has yet to gain popularity despite being introduced over 4 decades ago[141]. Primary reasons behind the lack of traction could be outcome variability and a lack of real-time validation of blood-brain barrier permeability. Initial studies have shown that dynamic contrast susceptibility (DSC) MRI defines catheter perfusion territory and contrast-enhanced images delineated OBBBO territory [141]. A first-in-human study by Zawadzki et al. demonstrated safety and feasibility of real-time MRI guidance for intra-arterial therapy delivery following OBBBO [142,143]. Authors emphasized that superselective IA delivery of therapy, in conjunction with real-time MRI guidance and validation, decreased volume of the enhancing mass, rapidly improved neurological status, and potentially improved survival in a rapidly declining patient with glioblastoma [142].

4.3.2 Liver oncology—Respiratory and cardiac motion affect abdominal organs to a greater extent than the central nervous system, requiring high temporal resolution. MRI can be used to ascertain not only spin thermal relaxation such as T1 and T2 relaxation times, and molecular electron cloud polarization, such as magnetic susceptibility, but also

contrast enhancement kinetics and water motion, such as perfusion and diffusion properties in one setting. MR monitoring of intra-arterial contrast infusions has demonstrated the ability to clearly demarcate tissue fed by the selected artery, providing insight into the impact of embolics administered via that vessel [144]. These advantages have prompted some groups to investigate use of MRI during endovascular oncologic treatments such as chemoembolization or radioembolization [145,146]; however, clinical applications have thus far mostly used coregistration of preprocedural MRI scans to intra-procedural cone beam CT. Nevertheless, coregistration of preoperative MRI to intraprocedural imaging is subject to errors such as misregistration, changes in the patient or disease process between the two scans, and variation from respiratory or cardiac motion. The development of MRI-conditional equipment could greatly aid in performing such interventions with real-time MRI guidance. One group has used intraprocedural transcatheter MRI perfusion imaging to assess chemoembolization endpoints in an angiography-MRI suite; though, the key procedural steps such as target vessel catheterization were performed using x-ray fluoroscopy [147]. As MRI biomarkers of treatment success become more established as surrogate markers of patient outcome, the advantages of MRI guidance for oncologic treatments will only increase.

4.4 Preclinical applications

Many endovascular interventional radiology applications have been tested *in vivo* in animal models, given the lack of clinically approved devices. Notable preclinical applications that could benefit from using MRI to quantitatively measure success are stroke embolectomy and tumor embolization. Recently, one group demonstrated a proof-of-concept performing a carotid embolectomy under MRI guidance in a swine stroke model [148]. This approach could be particularly valuable in acute ischemic stroke where intervention could be streamlined into one interventional suite, reducing treatment delays and allowing for intra-procedural evaluation of brain parenchyma viability, such that reperfusion therapy could be directed to living tissue and not at infarcted tissue [149]. Lillaney et al. demonstrated the ability to embolize renal arteries in a swine embolization model, additionally evaluating perfusion and flow pre- and post-procedure as imaging biomarkers [114]. Similar studies have been executed demonstrating renal artery embolization and hepatic artery drug infusion [150,151]. This approach could be particularly valuable in tumor embolization where new MR imaging techniques are being applied to evaluate tumor perfusion reduction during chemoembolization and have been shown to predict transplant free survival [147]. Other interventional radiology applications that have been tested in animal models include endovascular stenting of aortic aneurysms [152,153], stenting of descending thoracic dissections [154], angioplasty and stenting of arteries including carotid, renal and iliac arteries [82,155–157], inferior vena cava filter placement [158], and creation of porto-systemic shunts [159,160]. Preclinical interventional cardiology applications include coronary artery septum placement [161,162], pulmonary artery stenting [163], balloon angioplasty of aortic co-arctation [164], aortic valve placement [165] and septum occlusion [166,167]. Oncology applications have established small and large animal models for stem cell delivery to the CNS [168] as well as optimization of OBBBO with other intra-arterial therapies [141,169–171]. Finally, researchers have found an intersection between molecular MRI and endovascular interventions with chemical exchange saturation transfer (CEST) MR

contrast agents. Preclinical models to better assess OBBBO perfusion territory [172] and function as “label-free” theranostics following brain ischemia [173] have been identified in this field of research in addition to an expanding portfolio of MR contrast agents on the horizon[174].

5.0 Cost

Relatively little attention has been paid to this critical issue. Hall et al. explored the costs and benefits of MRI-guided brain tumor resections [175], concluding the potential costs of interventional MRI could be offset by improved health outcomes. Their work demonstrated that adults who had a brain tumor resection in an intraoperative MRI had a 54.9% shorter hospital length of stay compared to those who had resection performed in a conventional OR, showing a higher turnover rate and financial advantage to using MRI. Currently, the cost of a diagnostic MRI exam is typically 2–3 times more than that of a CT or ultrasound, and the increased cost is an area of significant scrutiny. Nonetheless, there have been efforts in recent years for a “Limited MRI” Current Procedural Terminology (CPT) code. This is an MRI scan with only a few essential, focused sequences, for a clinical indication that should have the best visualization on MRI. The reduced overall time in the MRI scan room (~15 minutes including set-up), in combination with the ability to avoid imaging modalities that are less specific, allow the overall cost to be lowered, such that the cost is on par with that of an ultrasound or CT scan [176]. This same concept could be applied to reduce the cost of interventional procedures; however, MRI-guided therapy must first thoroughly prove its cost effectiveness and value as a minimally invasive surgery over open surgery [177]. In body interventional radiology, biopsy and ablation CPT codes used for CT procedures have been applied to MRI-guided procedures [178]. Authors emphasized the importance of patients consulting with billing offices and their health insurance provider to predetermine out-of-pocket expenses or prior authorization requirements. Ultimately, demonstrating improved clinical outcomes, such as shorter length of hospital and rehabilitation stay and reduced disability in acute ischemic stroke, will drive reimbursement strategy and insurance coverage determination. Access to an interventional MRI unit may help other interventional procedures maximize use and demonstrate clinical value as a return on investment.

6.0 Conclusion

Interventional MRI represents the next era of diagnostic and therapeutic biomedical imaging. Significant limitations in current devices designed for use under x-ray guidance have driven development of an array of next-generation capital equipment, catheters and guidewires, and tracking techniques. Promising technological progress has been made to ensure patient safety and enhance MRI-guided endovascular procedures in real-time. As more MRI-safe technology reaches the market, dissemination of minimally invasive techniques throughout various medical specialties will follow at great benefit to operators and patients alike.

7.0 Expert opinion

MRI can provide crucial physiologic information which standard x-ray guidance cannot, such as diffusion and perfusion metrics, hemodynamics, and soft tissue characterization. In particular, the ability of MRI to precisely and confidently discriminate between living and dead or cancerous and noncancerous tissue could yield important benefits to patients if harnessed properly to better define targets during image-guided interventions. Yet, interventional fields of medicine have not transitioned away from x-ray fluoroscopic guidance.

Hesitance to adopt interventional MRI may stem from multiple root causes. Safety concerns arising from introduction of interventional devices into the MRI environment are relevant and will require careful characterization and consideration. Conversely, other trends in healthcare, such as greater availability of MRI-conditional devices and accessibility to MRI in general, may accelerate adoption and proliferation of MRI-safe environments in hospital settings. Low-field MRI scanners have been deployed to the patient bedside for point-of-care applications, which may also be able to provide improved patient access like prior open-bore configurations [179]. Additionally, new hospitals are increasingly being outfitted with MRI scanners within their interventional and operating suite environments. We expect that these trends will only further cement the centrality of MRI in management of many neurologic, cardiac, and oncologic diseases.

Another concern relates to the limited spatial and temporal resolution of interventional MRI sequences, presenting a challenge to device tracking in 3D space. Myriad techniques have been conceived to improve the imaging ecosystem [180], depending on whether an active, passive, or wireless resonant tracking strategy is pursued. Ongoing development of fast MRI pulse sequences, as well as routine high-fidelity coregistration of preoperative MRI with real-time intraoperative MRI, are expected to continue to improve over time and will further streamline procedural care [181].

Development of interventional devices that are safe and conspicuous in the MRI environment will likely shape the way that interventional MRI is adopted in the future. There are a wide variety of endovascular devices available in a physician’s armamentarium for fluoroscopically-guided interventions; the number of tools available for endovascular intervention under MRI guidance will be significantly less, at least initially. Once a broader selection of MRI-conditional and safe devices becomes available, diversification and larger scale utilization of interventional MRI may follow. While there are multiple types of devices under active investigation specifically indicated for interventional MRI, considerable regulatory hurdles exist prior to entering the market. The most straightforward avenue by which new devices can be approved is through substantial equivalence to commercial devices in a 510K clearance. In the case of novel tracking techniques, this will be a major challenge, as equivalent devices are scarce. The arduous regulatory process in the US, (nicknamed ‘Death Valley’ [182]) encourages more iterative design over paradigm-shifting technology, which may delay clinical translation. Therefore, translational research in conjunction with preclinical data will remain paramount in expanding the number of devices and procedures with utility for MRI-guided endovascular intervention. As combination

imaging suites become more prevalent, devices with multimodality visualization capabilities could be beneficial but have yet to be realized.

Technological advancements in single-use devices will act synergistically with those in capital equipment. Advanced RF transmission technologies like PTx coil arrays can enable use of standard guidewires, for example [77]. For these systems to be used in humans, on-board active SAR monitoring is needed. This area of research is active, having demonstrated *in vivo* success of dynamic RF-induced current control. Future steps are being taken to produce current measuring devices in a sterile format to complement pTx on conventional scanners. Robotic assistance may also enhance MRI-guided intervention, mitigating potential occupational hazards for operators. Future systems could further specialize for specific procedures or specialties, potentially with higher precision and cooperative control where there is real-time haptic feedback in conjunction with hands-on interfaces. Recent research suggests this is possible, with a shift towards fully MRI-safe platforms using non-metallic materials and pneumatic actuation.

Still, the most critical hurdle remains in justifying the costs associated with establishing interventional MRI suites. Bringing up an interventional system requires significant investment; thus thorough clinical advantage must be proven. Given the technical barriers and cost to implementing interventional MRI, future studies must go beyond proof-of-concept to demonstrate improved efficacy over other image guidance modalities such as x-ray fluoroscopy, ultrasound, or x-ray CT. By routinely implementing MRI guidance during cardiac electrophysiology intervention, oncologic intervention, ischemic stroke intervention, among other interventions, improved outcomes could further support these claims. These image-guided interventions, in particular, have evolved to become heavily dependent on preprocedural diagnostic MRI to define targets for treatment. If MRI guidance were integrated into the following procedural workflows, treatment could be streamlined with improved results. Perhaps in the future, interventional MRI scanners could see the most use in multi-room configurations where they can be maximally utilized during interventions or in parallel as diagnostic scanners. These suite designs could still greatly vary on a hospital basis depending on the application, surgeon, procedure being performed, and disease processes involved.

We anticipate a combination of factors leading to increased adoption of interventional MRI over the coming years. These include increased accessibility to MRI within healthcare systems, regulatory approval of single-use disposable MRI-conditional devices, clinical demonstration of MRI’s utility for management of cardiac, neurologic, and oncologic disease, continued development of real-time MRI tracking pulse sequences, and development of robotic tools to aid with the ergonomics of image-guided interventions. Financial and regulatory barriers in the healthcare system are expected to continue to limit rapid adoption of any technology, laying emphasis on the need for robust translational research efforts to ensure safety and efficacy.

Funding

This work was supported by the NIH under Grant R01 EB012031.

References

Papers of special note have been highlighted as:

* of interest

** of considerable interest

[1]. Higashida RT, Lahue BJ, Torbey MT, et al. Treatment of unruptured intracranial aneurysms: a nationwide assessment of effectiveness. AJNR Am J Neuroradiol. 2007;28:146–151. [PubMed: 17213445]

[2]. Bock M, Wacker FK. MR-guided intravascular interventions: Techniques and applications. J Magn Reson Imaging. 2008;27:326–338. [PubMed: 18219686] **Detailed review of tracking methods and applications of MRI-guided interventions.

[3]. Rudin S, Bednarek DR, Hoffmann KR. Endovascular image-guided interventions (EIGIs). Med Phys. 2008;35:301. [PubMed: 18293585]

[4]. Thomas DG, Davis CH, Ingram S, et al. Stereotaxic biopsy of the brain under MR imaging control. AJNR Am J Neuroradiol. 1986;7:161–163. [PubMed: 3082131]

[5]. Mueller PR, Stark DD, Simeone JF, et al. MR-guided aspiration biopsy: needle design and clinical trials. Radiology. 1986;161:605–609. [PubMed: 3786706]

[6]. Lufkin R, Teresi L, Hanafee W. New needle for MR-guided aspiration cytology of the head and neck. American Journal of Roentgenology. 1987;149:380–382. [PubMed: 3496765]

[7]. Van Sonnenberg E, Hajek PC, Baker LL, et al. Materials for MR- guided interventional radiology procedures: laboratory and clinical experience. 1986.

[8]. Köchli VD, McKinnon GC, Hofmann E, et al. Vascular interventions guided by ultrafast MR imaging: Evaluation of different materials. Magn Reson Med. 1994;31:309–314. [PubMed: 8057802]

[9]. Bakker CJ, Hoogeveen RM, Weber J, et al. Visualization of dedicated catheters using fast scanning techniques with potential for MR-guided vascular interventions. Magn Reson Med. 1996;36:816–820. [PubMed: 8946346]

[10]. Bakker CJ, Smits HF, Bos C, et al. MR-guided balloon angioplasty: In vitro demonstration of the potential of MRI for guiding, monitoring, and evaluating endovascular interventions. J Magn Reson Imaging. 1998;8:245–250. [PubMed: 9500288]

[11]. Kos S, Huegli R, Bongartz GM, et al. MR-guided endovascular interventions: a comprehensive review on techniques and applications. Eur Radiol. 2008;18:645–657. [PubMed: 18071710]

[12]. Saeed M, Hetts SW, English J, et al. MR fluoroscopy in vascular and cardiac interventions (review). Int J Cardiovasc Imaging. 2012;28:117–137. [PubMed: 21359519]

[13]. Lufkin RB, Gronemeyer DHW, Seibel RMM. Interventional MRI: update: Eur Radiol. 1997;7:S187–S200.

[14]. Grönemeyer D, Seibel R, Erbel R, et al. Equipment configuration and procedures: Preferences for interventional micro therapy. J Digit Imaging. 1996;9:81–96. [PubMed: 8734578]

[15]. Mislow JMK, Golby AJ, Black PM. Origins of Intraoperative MRI. Neurosurg Clin N Am. 2009;20:137–146. [PubMed: 19555875]

[16]. Schenck JF, Jolesz FA, Roemer PB, et al. Superconducting open-configuration MR imaging system for image-guided therapy. Radiology. 1995;195:805–814. [PubMed: 7754014]

[17]. Azmi H, Gibbons M, DeVito MC, et al. The interventional magnetic resonance imaging suite: Experience in the design, development, and implementation in a pre-existing radiology space and review of concepts. Surg Neurol Int. 2019;10:101. [PubMed: 31528439]

[18]. Hall WA, Liu H, Martin AJ, et al. Intraoperative Magnetic Resonance Imaging: Top Magn Reson Imaging. 2000;11:203–212. [PubMed: 11145212]

[19]. Foroglou N, Zamani A, Black P. Intra-operative MRI (iop-MR) for brain tumour surgery. Br J Neurosurg. 2009;23:14–22. [PubMed: 19234904]

[20]. Albayrak B, Samdani AF, Black PM. Intra-operative magnetic resonance imaging in neurosurgery. Acta Neurochir (Wien). 2004;146:543–557. [PubMed: 15168222]

[21]. Hoult DI, Saunders JK, Sutherland GR, et al. The engineering of an interventional MRI with a movable 1.5 Tesla magnet. J Magn Reson Imaging. 2001;13:78–86. [PubMed: 11169807]

[22]. Sutherland GR, Kaibara T, Louw D, et al. A mobile high-field magnetic resonance system for neurosurgery. J Neurosurg. 1999;91:804–813. [PubMed: 10541238]

[23]. Chen X, Xu B, Meng X, et al. Dual-room 1.5-T intraoperative magnetic resonance imaging suite with a movable magnet: implementation and preliminary experience. Neurosurg Rev. 2012;35:95–110. [PubMed: 21674146]

[24]. Ntoukas V, Krishnan R, Seifert V. THE NEW GENERATION POLESTAR N20 FOR CONVENTIONAL NEUROSURGICAL OPERATING ROOMS: A PRELIMINARY REPORT. Oper Neurosurg. 2008;62:82–90.

[25]. White MJ, Thornton JS, Hawkes DJ, et al. Design, Operation, and Safety of Single-Room Interventional MRI Suites: Practical Experience From Two Centers: Safety of Single-Room Interventional MRI. J Magn Reson Imaging. 2015;41:34–43. [PubMed: 24497105]

[26]. Faranesh AZ. The Interventional MRI Suite. ISMRM 24. 2016.

[27]. Golshan M, Sagara Y, Wexelman B, et al. Pilot Study to Evaluate Feasibility of Image-Guided Breast-Conserving Therapy in the Advanced Multimodal Image-Guided Operating (AMIGO) Suite. Ann Surg Oncol. 2014;21:3356–3357. [PubMed: 25047476]

[28]. Narsinh KH, Kilbride BF, Mueller K, et al. Combined Use of X-ray Angiography and Intraprocedural MRI Enables Tissue-based Decision Making Regarding Revascularization during Acute Ischemic Stroke Intervention. Radiology. 2021;299:167–176. [PubMed: 33560189] **First description of biplane x-ray angiography – 3.0T MRI suite used for clinical stroke treatment and intraprocedure decision-making. Accompanied by a contextualizing editorial.

[29]. Riederer SJ, Tasciyan T, Farzaneh F, et al. MR fluoroscopy: Technical feasibility. Magn Reson Med. 1988;8:1–15. [PubMed: 3173063] **First demonstration of real-time MRI frame rates using sliding window techniques to achieve “MR fluoroscopy”.

[30]. Wright RC, Riederer SJ, Farzaneh F, et al. Real-time MR fluoroscopic data acquisition and image reconstruction. Magn Reson Med. 1989;12:407–415. [PubMed: 2628689]

[31]. Tsao J, Kozerke S. MRI temporal acceleration techniques. J Magn Reson Imaging. 2012;36:543–560. [PubMed: 22903655]

[32]. Santos JM, Wright GA, Pauly JM. Flexible real-time magnetic resonance imaging framework. 26th Annu Int Conf IEEE Eng Med Biol Soc [Internet]. San Francisco, CA, USA: IEEE; 2004 [cited 2021 Oct 19]. p. 1048–1051. Available from: http://ieeexplore.ieee.org/document/1403343/.

[33]. Egger J, Tokuda J, Chauvin L, et al. Integration of the OpenIGTLink Network Protocol for image-guided therapy with the medical platform MeVisLab: Integration of the OpenIGTLink Protocol with the MeVisLab Platform. Int J Med Robot. 2012;8:282–290. [PubMed: 22374845]

[34]. Pintilie S, Biswas L, Anderson K, et al. Visualization Software for Real-time, Image-guided Therapeutics in Cardiovascular Interventions. CI2BM09 - MICCAI Workshop Cardiovasc Interv Imaging Biophys Model [Internet]. London, United Kingdom; 2009. p. 141–148. Available from: http://hal.inria.fr/inria-00417831.

[35]. Dominique F, Dupuis A, Gulani V, et al. Real-time acquisition, reconstruction and mixed-reality display system for 2D and 3D cardiac {MRI}. Proc Jt Annu Meet ISMRM-ESMRMB Paris Fr [Internet]. 2018. p. 598. Available from: http://indexsmart.mirasmart.com/ISMRM2018/PDFfiles/0598.html.

[36]. J B, G V, C R, et al. Robotic technology in cardiovascular medicine. Nat Rev Cardiol. 2014;11:266–275. [PubMed: 24663088]

[37]. Reichert A, Bock M, Vogele M, et al. GantryMate: A Modular MR-Compatible Assistance System for MR-Guided Needle Interventions. Tomography. 2019;5:266–273. [PubMed: 31245548]

[38]. Li G, Patel NA, Sharma K, et al. Body-Mounted Robotics for Interventional MRI Procedures. IEEE Trans Med Robot Bionics. 2020;2:557–560. [PubMed: 33778433]

[39]. Cleary K, Lim S, Jun C, et al. Robotically Assisted Long Bone Biopsy Under MRI Imaging. Acad Radiol. 2018;25:74–81. [PubMed: 29074334]

[40]. Kundrat D, Dagnino G, Kwok TMY, et al. An MR-Safe Endovascular Robotic Platform: Design, Control, and Ex-Vivo Evaluation. IEEE Trans Biomed Eng. 2021;68:3110–3121. [PubMed: 33705306] *Interesting MRI-safe, disposable robot for endovascular navigation.

[41]. Abdelaziz MEMK, Tian L, Hamady M, et al. X-ray to MR: the progress of flexible instruments for endovascular navigation. Prog Biomed Eng. 2021;3:032004.

[42]. Nitz WR, Oppelt A, Renz W, et al. On the heating of linear conductive structures as guide wires and catheters in interventional MRI. J Magn Reson Imaging. 2001;13:105–114. [PubMed: 11169811]

[43]. Martin AJ, Baek B, Acevedo-Bolton G, et al. MR imaging during endovascular procedures: An evaluation of the potential for catheter heating: Catheter Heating during MR Scanning. Magn Reson Med. 2009;61:45–53. [PubMed: 19097197]

[44]. Konings MK, Bartels LW, Smits HFM, et al. Heating Around Intravascular Guidewires by Resonating RF Waves. J Magn Reson Imaging. 2000;12:79–85. [PubMed: 10931567]

[45]. Yeung CJ, Susil RC, Atalar E. RF safety of wires in interventional MRI: Using a safety index. Magn Reson Med. 2002;47:187–193. [PubMed: 11754458]

[46]. Basar B, Rogers T, Ratnayaka K, et al. Segmented nitinol guidewires with stiffness-matched connectors for cardiovascular magnetic resonance catheterization: preserved mechanical performance and freedom from heating. J Cardiovasc Magn Reson. 2015;17:105. [PubMed: 26620420]

[47]. Yildirim KD, Basar B, Campbell-Washburn AE, et al. A cardiovascular magnetic resonance (CMR) safe metal braided catheter design for interventional CMR at 1.5 T: freedom from radiofrequency induced heating and preserved mechanical performance. J Cardiovasc Magn Reson. 2019;21:16. [PubMed: 30841903]

[48]. Gall K, Yakacki CM, Liu Y, et al. Thermomechanics of the shape memory effect in polymers for biomedical applications. J Biomed Mater Res A. 2005;73A:339–348.

[49]. Bell JA, Saikus CE, Ratnayaka K, et al. A deflectable guiding catheter for real-time MRI-guided interventions. J Magn Reson Imaging. 2012;

[50]. Lillaney P, Caton C, Martin AJ, et al. Comparing deflection measurements of a magnetically steerable catheter using optical imaging and MRI. Med Phys. 2014;

[51]. ISO 10555–1:2013 Intravascular catheters — Sterile and single-use catheters — Part 1: General requirements. 2013.

[52]. ISO 11070:2014 Sterile single-use intravascular introducers, dilators and guidewires. 2014.

[53]. Massmann A, Buecker A, Schneider GK. Glass-Fiber–based MR-safe Guidewire for MR Imaging–guided Endovascular Interventions: In Vitro and Preclinical in Vivo Feasibility Study. Radiology. 2017;284:541–551. [PubMed: 28301310]

[54]. Kos S, Huegli R, Hofmann E, et al. First Magnetic Resonance Imaging-Guided Aortic Stenting and Cava Filter Placement Using a Polyetheretherketone-Based Magnetic Resonance Imaging-Compatible Guidewire in Swine: Proof of Concept. Cardiovasc Intervent Radiol. 2009;32:514–521. [PubMed: 19115070]

[55]. Kos S, Huegli R, Hofmann E, et al. MR-compatible polyetheretherketone-based guide wire assisting MR-guided stenting of iliac and supraaortic arteries in swine: Feasibility study. Minim Invasive Ther Allied Technol. 2009;18:181–188. [PubMed: 19431070]

[56]. ASTM F2182 – 19e2 Standard Test Method for Measurement of Radio Frequency Induced Heating On or Near Passive Implants During Magnetic Resonance Imaging [Internet]. Available from: https://www.astm.org/Standards/F2182.htm.

[57]. ASTM F2052 – 15 Standard Test Method for Measurement of Magnetically Induced Displacement Force on Medical Devices in the Magnetic Resonance Environment [Internet]. Available from: https://www.astm.org/Standards/F2052.htm.

[58]. ASTM F2119 – 07(2013) Standard Test Method for Evaluation of MR Image Artifacts from Passive Implants [Internet]. [cited 2021 Jun 1]. Available from: https://www.astm.org/Standards/F2119.htm.

[59]. Hushek SG, Russell L, Moser RF, et al. Safety Protocols for Interventional MRI1. Acad Radiol. 2005;12:1143–1148. [PubMed: 16112514]

[60]. ASTM F2503 – 13 Standard Practice for Marking Medical Devices and Other Items for Safety in the Magnetic Resonance Environment [Internet]. Available from: https://www.astm.org/f2503-13.html.

[61]. Delfino JG, Woods TO. New Developments in Standards for MRI Safety Testing of Medical Devices. Curr Radiol Rep. 2016;4:28.

[62]. Tzifa A, Krombach GA, Krämer N, et al. Magnetic Resonance–Guided Cardiac Interventions Using Magnetic Resonance–Compatible Devices: A Preclinical Study and First-in-Man Congenital Interventions. Circ Cardiovasc Interv. 2010;3:585–592. [PubMed: 21098745]

[63]. Available from: http://www.marvistech.com.

[64]. Li X, Perotti LE, Martinez JA, et al. Real-time 3T MRI-guided cardiovascular catheterization in a porcine model using a glass-fiber epoxy-based guidewire. Deniz CM, editor. PLOS ONE. 2020;15:e0229711.

[65]. Available from: http://www.nano4imaging.com.

[66]. Overall WR, Pauly JM, Stang PP, et al. Ensuring safety of implanted devices under MRI using reversed RF polarization: Implant Safety Using Reversed Polarization. Magn Reson Med. 2010;64:823–833. [PubMed: 20593374]

[67]. Etezadi-Amoli M, Stang P, Kerr A, et al. Interventional device visualization with toroidal transceiver and optically coupled current sensor for radiofrequency safety monitoring: Transceiver and RF Sensor for Device Visualization. Magn Reson Med. 2015;73:1315–1327. [PubMed: 24691876]

[68]. Gudino N, Sonmez M, Yao Z, et al. Parallel transmit excitation at 1.5 T based on the minimization of a driving function for device heating: Optimized pTX RF excitation for device heating minimization. Med Phys. 2014;42:359–371.

[69]. Ladd ME, Quick HH, Debatin JF. Interventional MRA and intravascular imaging. J Magn Reson Imaging. 2000;12:534–546. [PubMed: 11042634]

[70]. Weiss S, Vernickel P, Schaeffter T, et al. Transmission line for improved RF safety of interventional devices. Magn Reson Med. 2005;54:182–189. [PubMed: 15968655]

[71]. Vernickel P, Schulz V, Weiss S, et al. A Safe Transmission Line for MRI. IEEE Trans Biomed Eng. 2005;52:1094–1102. [PubMed: 15977738]

[72]. Zanchi MG, Venook R, Pauly JM, et al. An Optically Coupled System for Quantitative Monitoring of MRI-Induced RF Currents Into Long Conductors. IEEE Trans Med Imaging. 2010;29:169–178. [PubMed: 19758855]

[73]. Yeung CJ, Susil RC, Atalar E. RF heating due to conductive wires during MRI depends on the phase distribution of the transmit field. Magn Reson Med. 2002;48:1096–1098. [PubMed: 12465125]

[74]. Yeung CJ, Karmarkar P, McVeigh ER. Minimizing RF heating of conducting wires in MRI. Magn Reson Med. 2007;58:1028–1034. [PubMed: 17969097]

[75]. Campbell-Washburn AE, Rogers T, Stine AM, et al. Right heart catheterization using metallic guidewires and low SAR cardiovascular magnetic resonance fluoroscopy at 1.5 Tesla: first in human experience. J Cardiovasc Magn Reson. 2018;20:41. [PubMed: 29925397]

[76]. Kolandaivelu A, Bruce CG, Ramasawmy R, et al. Native contrast visualization and tissue characterization of myocardial radiofrequency ablation and acetic acid chemoablation lesions at 0.55 T. J Cardiovasc Magn Reson. 2021;23:50. [PubMed: 33952312]

[77]. Godinez F, Scott G, Padormo F, et al. Safe guidewire visualization using the modes of a PTx transmit array MR system. Magn Reson Med. 2020;83:2343–2355. [PubMed: 31722119] *Attractive methods using parallel transmit to permit safe visualization of conventional guidewires under MRI guidance.

[78]. Wacker FK, Hillenbrand CM, Duerk JL, et al. MR-Guided Endovascular Interventions: Device Visualization, Tracking, Navigation, Clinical Applications, and Safety Aspects. Magn Reson Imaging Clin N Am. 2005;13:431–439. [PubMed: 16084411]

[79]. Settecase F, Martin AJ, Lillaney P, et al. Magnetic Resonance–Guided Passive Catheter Tracking for Endovascular Therapy. Magn Reson Imaging Clin N Am. 2015;23:591–605. [PubMed: 26499277]

[80]. Henk CB, Higgins CB, Saeed M. Endovascular interventional MRI. J Magn Reson Imaging. 2005;22:451–460. [PubMed: 16161076]

[81]. Patil S, Bieri O, Jhooti P, et al. Automatic slice positioning (ASP) for passive real-time tracking of interventional devices using projection-reconstruction imaging with echo-dephasing (PRIDE): Passive Marker Tracking Using PRIDE. Magn Reson Med. 2009;62:935–942. [PubMed: 19585605]

[82]. Buecker A, Neuerburg JM, Adam GB, et al. Real-time MR fluoroscopy for MR-guided iliac artery stent placement. J Magn Reson Imaging. 2000;12:616–622. [PubMed: 11042645]

[83]. Buecker A, Adam GB, Neuerburg JM, et al. Simultaneous real-time visualization of the catheter tip and vascular anatomy for MR-guided PTA of iliac arteries in an animal model. J Magn Reson Imaging. 2002;16:201–208. [PubMed: 12203769]

[84]. Razavi R, Hill DL, Keevil SF, et al. Cardiac catheterisation guided by MRI in children and adults with congenital heart disease. The Lancet. 2003;362:1877–1882.

[85]. Muthurangu V, Taylor A, Andriantsimiavona R, et al. Novel Method of Quantifying Pulmonary Vascular Resistance by Use of Simultaneous Invasive Pressure Monitoring and Phase-Contrast Magnetic Resonance Flow. Circulation. 2004;110:826–834. [PubMed: 15302793]

[86]. Pushparajah K, Tzifa A, Bell A, et al. Cardiovascular Magnetic Resonance catheterization derived pulmonary vascular resistance and medium-term outcomes in congenital heart disease. J Cardiovasc Magn Reson. 2015;17:28. [PubMed: 25890289]

[87]. Ratnayaka K, Faranesh AZ, Hansen MS, et al. Real-time MRI-guided right heart catheterization in adults using passive catheters. Eur Heart J. 2013;34:380–389. [PubMed: 22855740]

[88]. Dumoulin CL, Souza SP, Darrow RD. Real-time position monitoring of invasive devices using magnetic resonance. Magn Reson Med. 1993;29:411–415. [PubMed: 8450752] *First demonstration of MRI tracking sequences of active markers.

[89]. Glowinski A, Kursch J, Adam G, et al. Device visualization for interventional MRI using local magnetic fields: basic theory and its application to catheter visualization. IEEE Trans Med Imaging. 1998;17:786–793. [PubMed: 9874303]

[90]. Konings MK, Bartels LW, van Swol CFP, et al. Development of an MR-safe tracking catheter with a laser-driven tip coil. J Magn Reson Imaging. 2001;13:131–135. [PubMed: 11169815]

[91]. Dumoulin CL, Mallozzi RP, Darrow RD, et al. Phase-field dithering for active catheter tracking. Magn Reson Med. 2010;63:1398–1403. [PubMed: 20432311]

[92]. Ratnayaka K, Saikus CE, Faranesh AZ, et al. Closed-Chest Transthoracic Magnetic Resonance Imaging-Guided Ventricular Septal Defect Closure in Swine. JACC Cardiovasc Interv. 2011;4:1326–1334. [PubMed: 22192373]

[93]. Yildirim DK, Bruce C, Uzun D, et al. A 20-gauge active needle design with thin-film printed circuitry for interventional MRI at 0.55T. Magn Reson Med. 2021;86:1786–1801. [PubMed: 33860962]

[94]. Chubb H, King's College London, London, UK, Williams SE, et al. Cardiac Electrophysiology Under MRI Guidance: an Emerging Technology. Arrhythmia Electrophysiol Rev. 2017;6:85. *First in-human study demonstrating feasibility of active catheters.

[95]. Mukherjee RK, Roujol S, Chubb H, et al. Epicardial electroanatomical mapping, radiofrequency ablation, and lesion imaging in the porcine left ventricle under real-time magnetic resonance imaging guidance—an in vivo feasibility study. EP Eur. 2018;20:f254–f262.

[96]. Dukkipati SR, Mallozzi R, Schmidt EJ, et al. Electroanatomic Mapping of the Left Ventricle in a Porcine Model of Chronic Myocardial Infarction With Magnetic Resonance–Based Catheter Tracking. Circulation. 2008;118:853–862. [PubMed: 18678773]

[97]. Yaras YS, Yildirim DK, Herzka DA, et al. Real-time device tracking under MRI using an acousto-optic active marker. Magn Reson Med. 2021;85:2904–2914. [PubMed: 33347642]

[98]. Krug J, Will K, Rose G. Simulation and experimental validation of resonant electric markers used for medical device tracking in magnetic resonance imaging. 2010 Annu Int Conf IEEE Eng Med Biol [Internet]. Buenos Aires: IEEE; 2010 [cited 2021 Oct 19]. p. 1878–1881. Available from: http://ieeexplore.ieee.org/document/5627137/.

[99]. Burl M, Coutts GA, Young IR. Tuned fiducial markers to identify body locations with minimal perturbation of tissue magnetization. Magn Reson Med. 1996;36:491–493. [PubMed: 8875424]

[100]. Rube MA, Holbrook AB, Cox BF, et al. Wireless MR tracking of interventional devices using phase-field dithering and projection reconstruction. Magn Reson Imaging. 2014;32:693–701. [PubMed: 24721007]

[101]. Celik H, Ulutürk A, Talı T, et al. A catheter tracking method using reverse polarization for MR-guided interventions. Magn Reson Med. 2007;58:1224–1231. [PubMed: 18046701]

[102]. Quick HH, Zenge MO, Kuehl H, et al. Interventional magnetic resonance angiography with no strings attached: Wireless active catheter visualization. Magn Reson Med. 2005;53:446–455. [PubMed: 15678524]

[103]. Kuehne T, Fahrig R, Butts K. Pair of resonant fiducial markers for localization of endovascular catheters at all catheter orientations. J Magn Reson Imaging. 2003;17:620–624. [PubMed: 12720274]

[104]. Ellersiek D, Fassbender H, Bruners P, et al. A monolithically fabricated flexible resonant circuit for catheter tracking in magnetic resonance imaging☆. Sens Actuators B Chem. 2010;144:432–436.

[105]. Thorne B, Lillaney P, Losey A, et al. Micro Resonant Marker for Endovascular Catheter Tracking in Interventional MRI: In Vitro Imaging at 3T. J Magn Reson Imaging Proc Intl Soc Reson Med Proc Intl Soc Mag Reson Med. 2014. p. 620–624.

[106]. Thorne B, Lillaney P, Losey A, et al. Omnidirectional mri catheter resonator and related systems, methods, and devices.

[107]. Jordan CD, Thorne BRH, Wadhwa A, et al. Wireless Resonant Circuits Printed Using Aerosol Jet Deposition for MRI Catheter Tracking. IEEE Trans Biomed Eng. 2020;67:876–882. [PubMed: 31247538]

[108]. Kaiser M, Detert M, Rube MA, et al. Resonant marker design and fabrication techniques for device visualization during interventional magnetic resonance imaging. Biomed Eng Biomed Tech [Internet]. 2015 [cited 2021 Oct 19];60. Available from: 10.1515/bmt-2013-0097/html.

[109]. Cheung C-L, Ho JD-L, Vardhanabhuti V, et al. Design and Fabrication of Wireless Multilayer Tracking Marker for Intraoperative MRI-Guided Interventions. IEEEASME Trans Mechatron. 2020;25:1016–1025.

[110]. Muller L, Saeed M, Wilson MW, et al. Remote control catheter navigation: options for guidance under MRI. J Cardiovasc Magn Reson. 2012;14:33. [PubMed: 22655535] *Review on remote controlled/steerable catheters.

[111]. Clogenson HCM, van Lith JY, Dankelman J, et al. Multi-selective catheter for MR-guided endovascular interventions. Med Eng Phys. 2015;37:623–630. [PubMed: 25937614]

[112]. Gosselin FP, Lalande V, Martel S. Characterization of the deflections of a catheter steered using a magnetic resonance imaging system: Deflections of a catheter steered using MRI System. Med Phys. 2011;38:4994–5002. [PubMed: 21978043] *First demonstration of a steerable catheter tipped with ferromagnetic spheres.

[113]. Heunis C, Sikorski J, Misra S. Flexible Instruments for Endovascular Interventions: Improved Magnetic Steering, Actuation, and Image-Guided Surgical Instruments. IEEE Robot Autom Mag. 2018;25:71–82.

[114]. Lillaney PV, Yang JK, Losey AD, et al. Endovascular MR-guided Renal Embolization by Using a Magnetically Assisted Remote-controlled Catheter System. Radiology. 2016;281:219–228. [PubMed: 27019290]

[115]. Hetts SW, Saeed M, Martin AJ, et al. Endovascular Catheter for Magnetic Navigation under MR Imaging Guidance: Evaluation of Safety In Vivo at 1.5T. Am J Neuroradiol. 2013;34:2083–2091. [PubMed: 23846795]

[116]. Liu T, Poirot NL, Franson D, et al. Modeling and Validation of the Three-Dimensional Deflection of an MRI-Compatible Magnetically Actuated Steerable Catheter. IEEE Trans Biomed Eng. 2016;63:2142–2154. [PubMed: 26731519]

[117]. Liu T, Jackson R, Franson D, et al. Iterative Jacobian-Based Inverse Kinematics and Open-Loop Control of an MRI-Guided Magnetically Actuated Steerable Catheter System. IEEEASME Trans Mechatron. 2017;22:1765–1776.

[118]. Gudino N, Heilman JA, Derakhshan JJ, et al. Control of intravascular catheters using an array of active steering coils: Controllable catheter with an array of steering coils. Med Phys. 2011;38:4215–4224. [PubMed: 21859023]

[119]. Mukherjee RK, Chubb H, Roujol S, et al. Advances in Real-Time MRI–Guided Electrophysiology. Curr Cardiovasc Imaging Rep. 2019;12:6. [PubMed: 31501689]

[120]. Rasche V, Holz D, Köhler J, et al. Catheter tracking using continuous radial MRI. Magn Reson Med. 1997;37:963–968. [PubMed: 9178250]

[121]. Rasche V, Proksa R, Sinkus R, et al. Resampling of data between arbitrary grids using convolution interpolation. IEEE Trans Med Imaging. 2002;18:385–392.

[122]. Schaeffter T, Weiss S, Eggers H, et al. Projection reconstruction balanced fast field echo for interactive real-time cardiac imaging. Magn Reson Med. 2001;46:1238–1241. [PubMed: 11746592]

[123]. Bock M, Volz S, Zühlsdorff S, et al. MR-guided intravascular procedures: Real-time parameter control and automated slice positioning with active tracking coils: Real-Time MRI for MR-Guided Interventions. J Magn Reson Imaging. 2004;19:580–589. [PubMed: 15112307]

[124]. Martin AJ, Lillaney P, Saeed M, et al. Digital subtraction MR angiography roadmapping for magnetic steerable catheter tracking: Digital Subtraction MR Angiography Roadmapping. J Magn Reson Imaging. 2015;41:1157–1162. [PubMed: 24797218]

[125]. Zhang K, Maier F, Krafft AJ, et al. Tracking of an interventional catheter with a ferromagnetic tip using dual-echo projections. J Magn Reson. 2013;234:176–183. [PubMed: 23892103]

[126]. Seppenwoolde J-H, Viergever MA, Bakker CJG. Passive tracking exploiting local signal conservation: The white marker phenomenon. Magn Reson Med. 2003;50:784–790. [PubMed: 14523965]

[127]. Velasco Forte MN, Pushparajah K, Schaeffter T, et al. Improved passive catheter tracking with positive contrast for CMR-guided cardiac catheterization using partial saturation (pSAT). J Cardiovasc Magn Reson. 2017;19:60. [PubMed: 28806996]

[128]. Ratnayaka K, Faranesh AZ, Guttman MA, et al. Interventional cardiovascular magnetic resonance: still tantalizing. J Cardiovasc Magn Reson. 2008;10:62. [PubMed: 19114017]

[129]. Pushparajah K, Chubb H, Razavi R. MR-guided Cardiac Interventions. Top Magn Reson Imaging. 2018;27:115–128. [PubMed: 29870464]

[130]. Campbell-Washburn AE, Tavallaei MA, Pop M, et al. Real-time MRI guidance of cardiac interventions: Real-Time Cardiac MRI Interventions. J Magn Reson Imaging. 2017;46:935–950. [PubMed: 28493526]

[131]. Ratnayaka K, Kanter JP, Faranesh AZ, et al. Radiation-free CMR diagnostic heart catheterization in children. J Cardiovasc Magn Reson. 2017;19:65. [PubMed: 28874164]

[132]. Kuo L, Liang JJ, Han Y, et al. Association of septal late gadolinium enhancement on cardiac magnetic resonance with ventricular tachycardia ablation targets in nonischemic cardiomyopathy. J Cardiovasc Electrophysiol. 2020;31:3262–3276. [PubMed: 33070414]

[133]. Lloyd DF, Van AJ, Murgasova M, et al. Insights from comprehensive fetal cardiovascular MRI assessment using 3D motion–correction and metric–optimised gated phase contrast in cases of suspected coarctation of the aorta. 2017. p. 3261.

[134]. Toupin S, Bour P, Lepetit-Coiffé M, et al. Feasibility of real-time MR thermal dose mapping for predicting radiofrequency ablation outcome in the myocardium in vivo. J Cardiovasc Magn Reson. 2017;19:14. [PubMed: 28143574]

[135]. Sorensen TS, Atkinson D, Schaeffter T, et al. Real-Time Reconstruction of Sensitivity Encoded Radial Magnetic Resonance Imaging Using a Graphics Processing Unit. IEEE Trans Med Imaging. 2009;28:1974–1985. [PubMed: 19628452]

[136]. Hansen MS, Sørensen TS. Gadgetron: An open source framework for medical image reconstruction: Gadgetron. Magn Reson Med. 2013;69:1768–1776. [PubMed: 22791598]

[137]. Manke C, Nitz WR, Djavidani B, et al. MR Imaging-guided Stent Placement in Iliac Arterial Stenoses: A Feasibility Study. Radiology. 2001;219:527–534. [PubMed: 11323483]

[138]. Paetzel C, Zorger N, Bachthaler M, et al. Magnetic Resonance-Guided Percutaneous Angioplasty of Femoral and Popliteal Artery Stenoses Using Real-Time Imaging and Intra-

arterial Contrast-Enhanced Magnetic Resonance Angiography. Invest Radiol. 2005;40:257–262. [PubMed: 15829822]

[139]. Paetzel C, Zorger N, Bachthaler M, et al. Magnetic resonance-guided percutaneous angioplasty of femoral and popliteal artery stenoses using real-time imaging and intra-arterial contrast-enhanced magnetic resonance angiography. Invest Radiol. 2005;40:257–262. [PubMed: 15829822]

[140]. Fleg JL, Stone GW, Fayad ZA, et al. Detection of High-Risk Atherosclerotic Plaque. JACC Cardiovasc Imaging. 2012;5:941–955. [PubMed: 22974808]

[141]. Janowski M, Walczak P, Pearl MS. Predicting and optimizing the territory of blood-brain barrier opening by superselective intra-arterial cerebral infusion under dynamic susceptibility contrast MRI guidance. J Cereb Blood Flow Metab Off J Int Soc Cereb Blood Flow Metab. 2016;36:569–575.

[142]. Zawadzki M, Walecki J, Kostkiewicz B, et al. Real-time MRI guidance for intra-arterial drug delivery in a patient with a brain tumor: technical note. BMJ Case Rep. 2019;12:e014469.

[143]. Zawadzki M, Walecki J, Kostkiewicz B, et al. Follow-up of intra-arterial delivery of bevacizumab for treatment of butterfly glioblastoma in patient with first-in-human, real-time MRI-guided intra-arterial neurointervention. J Neurointerventional Surg. 2021;13:1037–1039.

[144]. Martin AJ, Cha S, Higashida RT, et al. Assessment of Vasculature of Meningiomas and the Effects of Embolization with Intra-arterial MR Perfusion Imaging: A Feasibility Study. Am J Neuroradiol. 2007;28:1771–1777. [PubMed: 17885240]

[145]. Roosen J, Arntz MJ, Janssen MJR, et al. Development of an MRI-Guided Approach to Selective Internal Radiation Therapy Using Holmium-166 Microspheres. Cancers. 2021;13:5462. [PubMed: 34771626]

[146]. Chen SR, Chen MM, Ene C, et al. Perfusion-guided endovascular super-selective intra-arterial infusion for treatment of malignant brain tumors. J Neurointerventional Surg. 2021;neurintsurg-2021–018190.

[147]. Wang D, Gaba RC, Jin B, et al. Perfusion reduction at transcatheter intraarterial perfusion MR imaging: a promising intraprocedural biomarker to predict transplant-free survival during chemoembolization of hepatocellular carcinoma. Radiology. 2014;272:587–597. [PubMed: 24678859]

[148]. Yang JK, Cote AM, Jordan CD, et al. Interventional magnetic resonance imaging guided carotid embolectomy using a novel resonant marker catheter: demonstration of preclinical feasibility. Biomed Microdevices. 2017;19:88. [PubMed: 28948399]

[149]. Khatri P, Yeatts SD, Mazighi M, et al. Time to angiographic reperfusion and clinical outcome after acute ischaemic stroke: an analysis of data from the Interventional Management of Stroke (IMS III) phase 3 trial. Lancet Neurol. 2014;13:567–574. [PubMed: 24784550]

[150]. Fink C, Bock M, Umathum R, et al. Renal Embolization: Feasibility of Magnetic Resonance-Guidance Using Active Catheter Tracking and Intraarterial Magnetic Resonance Angiography. Invest Radiol. 2004;39:111–119. [PubMed: 14734926]

[151]. Seppenwoolde J-H, Bartels LW, van der Weide R, et al. Fully MR-guided hepatic artery catheterization for selective drug delivery: A feasibility study in pigs. J Magn Reson Imaging. 2006;23:123–129. [PubMed: 16374883]

[152]. Raman VK, Karmarkar PV, Guttman MA, et al. Real-Time Magnetic Resonance-Guided Endovascular Repair of Experimental Abdominal Aortic Aneurysm in Swine. J Am Coll Cardiol. 2005;45:2069–2077. [PubMed: 15963411]

[153]. Mahnken AH, Chalabi K, Jalali F, et al. Magnetic Resonance–guided Placement of Aortic Stents Grafts: Feasibility with Real-Time Magnetic Resonance Fluoroscopy. J Vasc Interv Radiol. 2004;15:189–195. [PubMed: 14963188]

[154]. Eggebrecht H, Kühl H, Kaiser GM, et al. Feasibility of real-time magnetic resonance-guided stent-graft placement in a swine model of descending aortic dissection. Eur Heart J. 2006;27:613–620. [PubMed: 16431874]

[155]. Feng L, Dumoulin CL, Dashnaw S, et al. Transfemoral Catheterization of Carotid Arteries with Real-time MR Imaging Guidance in Pigs. Radiology. 2005;234:551–557. [PubMed: 15591433]

[156]. Elgort DR, Hillenbrand CM, Zhang S, et al. Image-guided and -monitored renal artery stenting using only MRI. J Magn Reson Imaging. 2006;23:619–627. [PubMed: 16555228]

[157]. Omary RA, Gehl JA, Schirf BE, et al. MR Imaging– versus Conventional X-ray Fluoroscopy–guided Renal Angioplasty in Swine: Prospective Randomized Comparison. Radiology. 2006;238:489–496. [PubMed: 16436813]

[158]. Bücker A, Neuerburg JM, Adam GB, et al. Real-time MR Guidance for Inferior Vena Cava Filter Placement in an Animal Model. J Vasc Interv Radiol. 2001;12:753–756. [PubMed: 11389228]

[159]. Arepally A, Karmarkar PV, Qian D, et al. Evaluation of MR/Fluoroscopy–guided Portosystemic Shunt Creation in a Swine Model. J Vasc Interv Radiol. 2006;17:1165–1173. [PubMed: 16868170]

[160]. Kee ST, Rhee JS, Butts K, et al. MR-guided Transjugular Portosystemic Shunt Placement in a Swine Model. J Vasc Interv Radiol. 1999;10:529–535. [PubMed: 10357476]

[161]. Spuentrup E, Ruebben A, Schaeffter T, et al. Magnetic Resonance–Guided Coronary Artery Stent Placement in a Swine Model. Circulation. 2002;105:874–879. [PubMed: 11854130]

[162]. Serfaty J-M, Yang X, Foo TK, et al. MRI-guided coronary catheterization and PTCA: A feasibility study on a dog model. Magn Reson Med. 2003;49:258–263. [PubMed: 12541245]

[163]. Kuehne T, Saeed M, Higgins CB, et al. Endovascular Stents in Pulmonary Valve and Artery in Swine: Feasibility Study of MR Imaging–guided Deployment and Postinterventional Assessment. Radiology. 2003;226:475–481. [PubMed: 12563142]

[164]. Krueger JJ, Ewert P, Yilmaz S, et al. Magnetic Resonance Imaging–Guided Balloon Angioplasty of Coarctation of the Aorta: A Pilot Study. Circulation. 2006;113:1093–1100. [PubMed: 16490822]

[165]. Kuehne T, Yilmaz S, Meinus C, et al. Magnetic resonance imaging-guided transcatheter implantation of a prosthetic valve in aortic valve position: J Am Coll Cardiol. 2004;44:2247–2249. [PubMed: 15582324]

[166]. Buecker A, Spuentrup E, Grabitz R, et al. Magnetic resonance-guided placement of atrial septal closure device in animal model of patent foramen ovale. Circulation. 2002;106:511–515. [PubMed: 12135954]

[167]. Ewert P, Berger F, Daehnert I, et al. Transcatheter Closure of Atrial Septal Defects Without Fluoroscopy: Feasibility of a New Method. Circulation. 2000;101:847–849. [PubMed: 10694522]

[168]. Walczak P, Wojtkiewicz J, Nowakowski A, et al. Real-time MRI for precise and predictable intra-arterial stem cell delivery to the central nervous system. J Cereb Blood Flow Metab Off J Int Soc Cereb Blood Flow Metab. 2017;37:2346–2358.

[169]. Chu C, Liu G, Janowski M, et al. Real-Time MRI Guidance for Reproducible Hyperosmolar Opening of the Blood-Brain Barrier in Mice. Front Neurol. 2018;9:921. [PubMed: 30416485]

[170]. Chu C, Jablonska A, Lesniak WG, et al. Optimization of osmotic blood-brain barrier opening to enable intravital microscopy studies on drug delivery in mouse cortex. J Control Release Off J Control Release Soc. 2020;317:312–321.

[171]. Chu C, Jablonska A, Gao Y, et al. Hyperosmolar blood-brain barrier opening using intra-arterial injection of hyperosmotic mannitol in mice under real-time MRI guidance. Nat Protoc. 2022;17:76–94. [PubMed: 34903870]

[172]. Song X, Walczak P, He X, et al. Salicylic acid analogues as chemical exchange saturation transfer MRI contrast agents for the assessment of brain perfusion territory and blood-brain barrier opening after intra-arterial infusion. J Cereb Blood Flow Metab Off J Int Soc Cereb Blood Flow Metab. 2016;36:1186–1194.

[173]. Liu H, Jablonska A, Li Y, et al. Label-free CEST MRI Detection of Citicoline-Liposome Drug Delivery in Ischemic Stroke. Theranostics. 2016;6:1588–1600. [PubMed: 27446492]

[174]. Chen L, Liu J, Chu C, et al. Deuterium oxide as a contrast medium for real-time MRI-guided endovascular neurointervention. Theranostics. 2021;11:6240–6250. [PubMed: 33995656]

[175]. Hall WA, Kowalik K, Liu H, et al. Costs and Benefits of Intraoperative MR-Guided Brain Tumor Resection. In: Bernays RL, Imhof H-G, Yonekawa Y, editors. Intraoperative Imaging

Neurosurg [Internet]. Vienna: Springer Vienna; 2003 [cited 2022 Feb 9]. p. 137–142. Available from: 10.1007/978-3-7091-6043-5_19.

[176]. Pooler BD, Hernando D, Reeder SB. Clinical Implementation of a Focused MRI Protocol for Hepatic Fat and Iron Quantification. Am J Roentgenol. 2019;213:90–95. [PubMed: 30917020]

[177]. van Beek EJR, Kuhl C, Anzai Y, et al. Value of MRI in medicine: More than just another test? J Magn Reson Imaging. 2019;49:e14–e25. [PubMed: 30145852]

[178]. Thompson SM, Gorny KR, Koepsel EMK, et al. Body Interventional MRI for Diagnostic and Interventional Radiologists: Current Practice and Future Prospects. RadioGraphics. 2021;41:1785–1801. [PubMed: 34597216] **Current, in-depth review of interventional MRI techniques, technology, safety considerations, and applications in body interventional radiology.

[179]. Bhat SS, Fernandes TT, Poojar P, et al. Low-Field MRI of Stroke: Challenges and Opportunities. J Magn Reson Imaging. 2021;54:372–390. [PubMed: 32827173]

[180]. Ciske BR, Speidel MA, Raval AN. Improving the cardiac cath-lab interventional imaging eco-system. Transl Pediatr. 2018;7:1–4. [PubMed: 29441275]

[181]. Gao X, Navkar NV, Shah DJ, et al. Intraoperative registration of preoperative 4D cardiac anatomy with real-time MR images. 2012 IEEE 12th Int Conf Bioinforma Bioeng BIBE [Internet]. Larnaca, Cyprus: IEEE; 2012 [cited 2021 Nov 15]. p. 583–588. Available from: http://ieeexplore.ieee.org/document/6399737/.

[182]. Bottomley PA. Barriers to technology translation in magnetic resonance to medicine. Magn Reson Mater Phys Biol Med. 2021;34:643–647.

Article Highlights

- Interventional MRI possesses unique benefits over standard x-ray fluoroscopy including superior soft-tissue contrast, no ionizing radiation, and measurement of quantitative biomarkers.
- Due to the significant technical effort and expertise needed, MRI-guided endovascular interventions are only recommended for situations in which MRI provides a significant advantage over other modalities.
- Current commercially available interventional devices lack MRI compatibility and safety profiles. Key characteristics must include ability to visualize the distal tip without sacrificing MRI safety and mechanical performance.
- Clinical adoption of interventional MRI requires future generations of MRI-conditional and MRI-safe devices to facilitate better tracking and treatment in real-time.

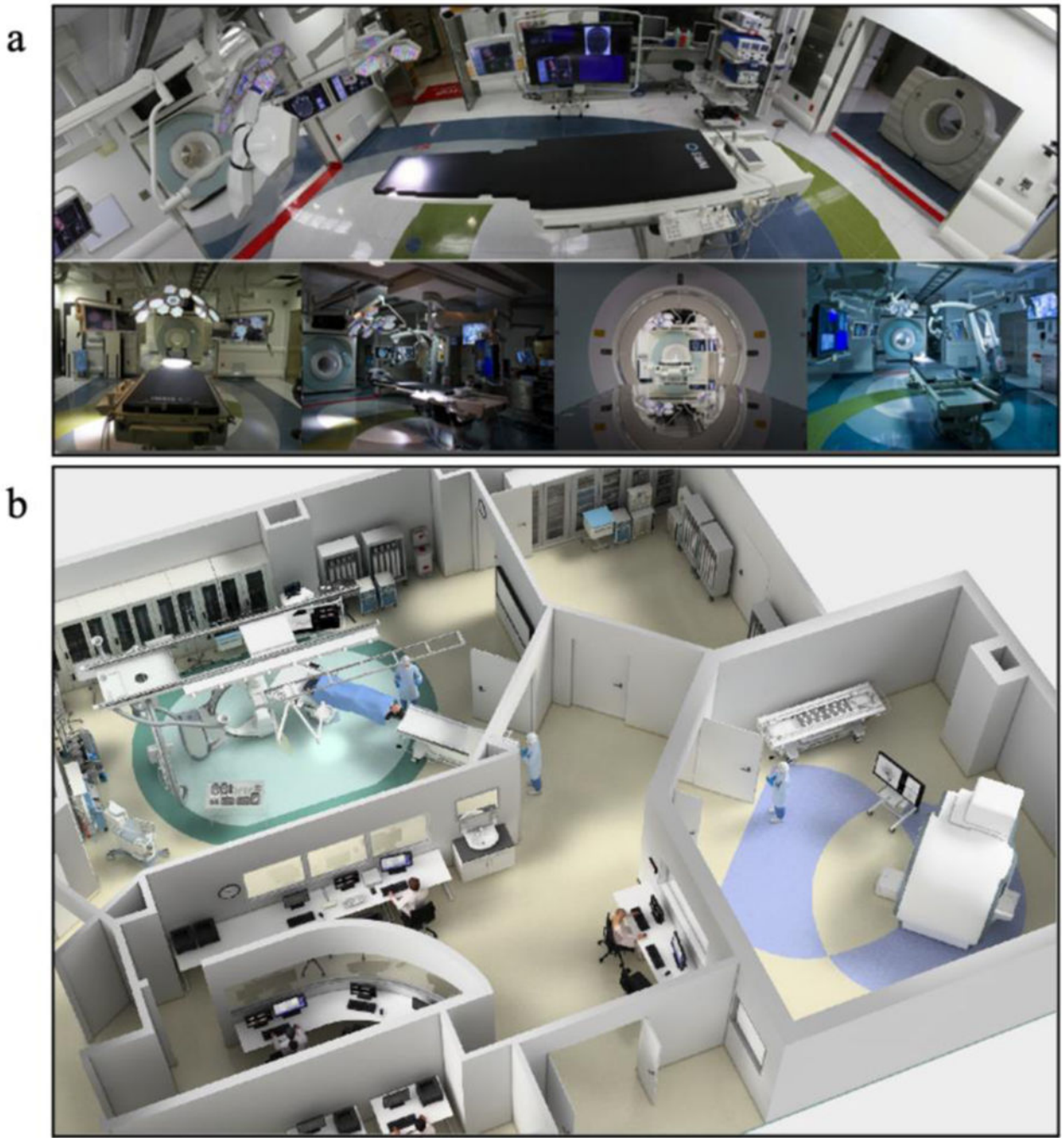

Figure 1.
Current interventional MRI suites often combine with other imaging modalities. a) The Brigham and Women's Hospital's AMIGO Suite combines a PET/CT, x-ray fluoroscopy table, and a 3.0T (image from https://ncigt.org/amigo), b) Rendering of Zuckerberg San Francisco General Hospital's AMR Suite Magnetom Skyra 3.0T MRI and Artis Q biplane angiographic system (image courtesy of Siemens Healthcare GmbH).

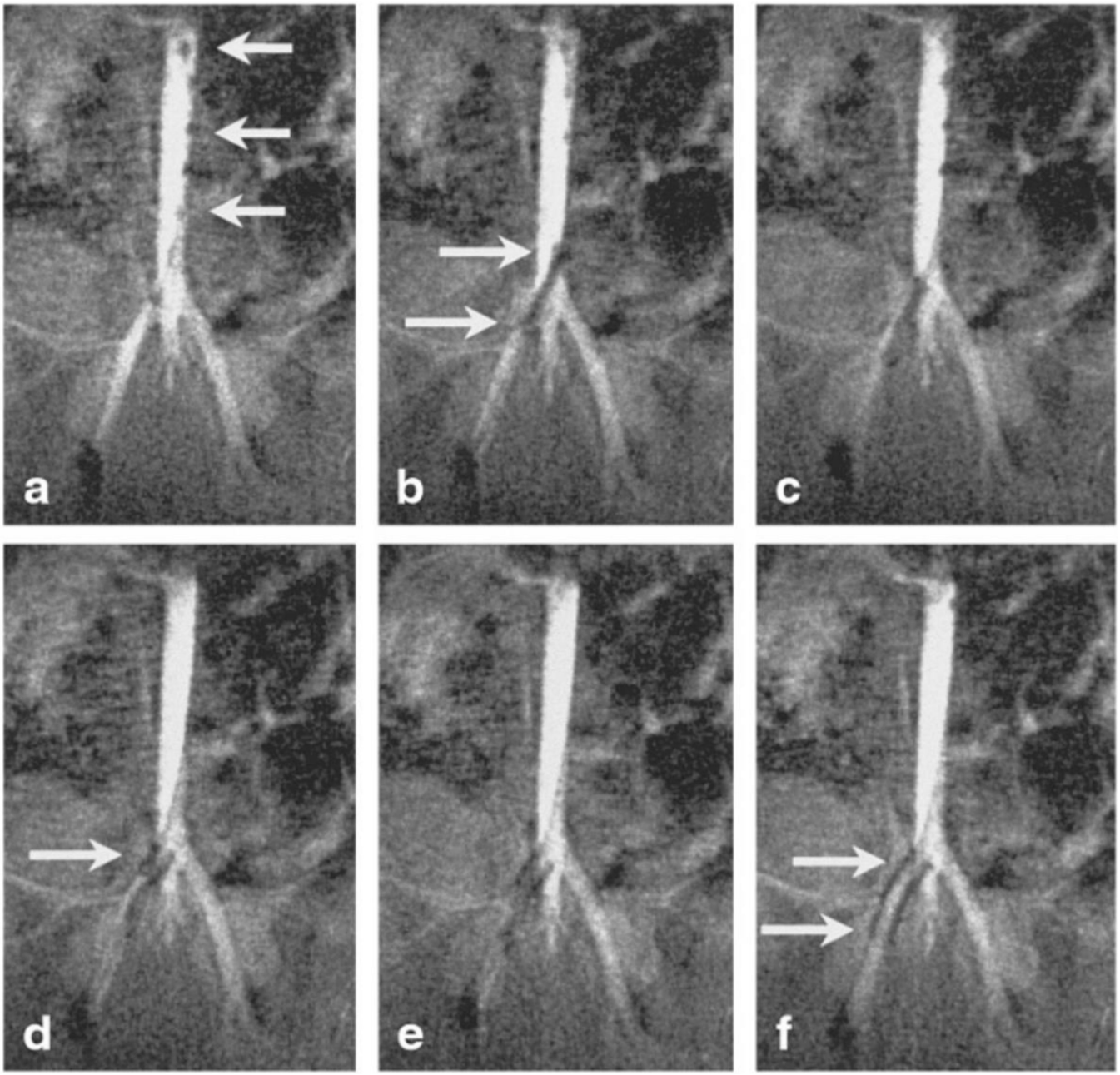

Figure 2.

MRI-guided iliac artery stent placement using Dy-doped catheters. a) Visualization of Dy markers (arrows) along the nonmetallic wire. b) The catheter-mounted ZA stent (arrows) positioned in the aorta c) The stent withdrawn to the position of deployment, and d,e) Stent deployment in real-time. f) Fully deployed stent (arrows) is shown [49].

Dy = Dysprosium

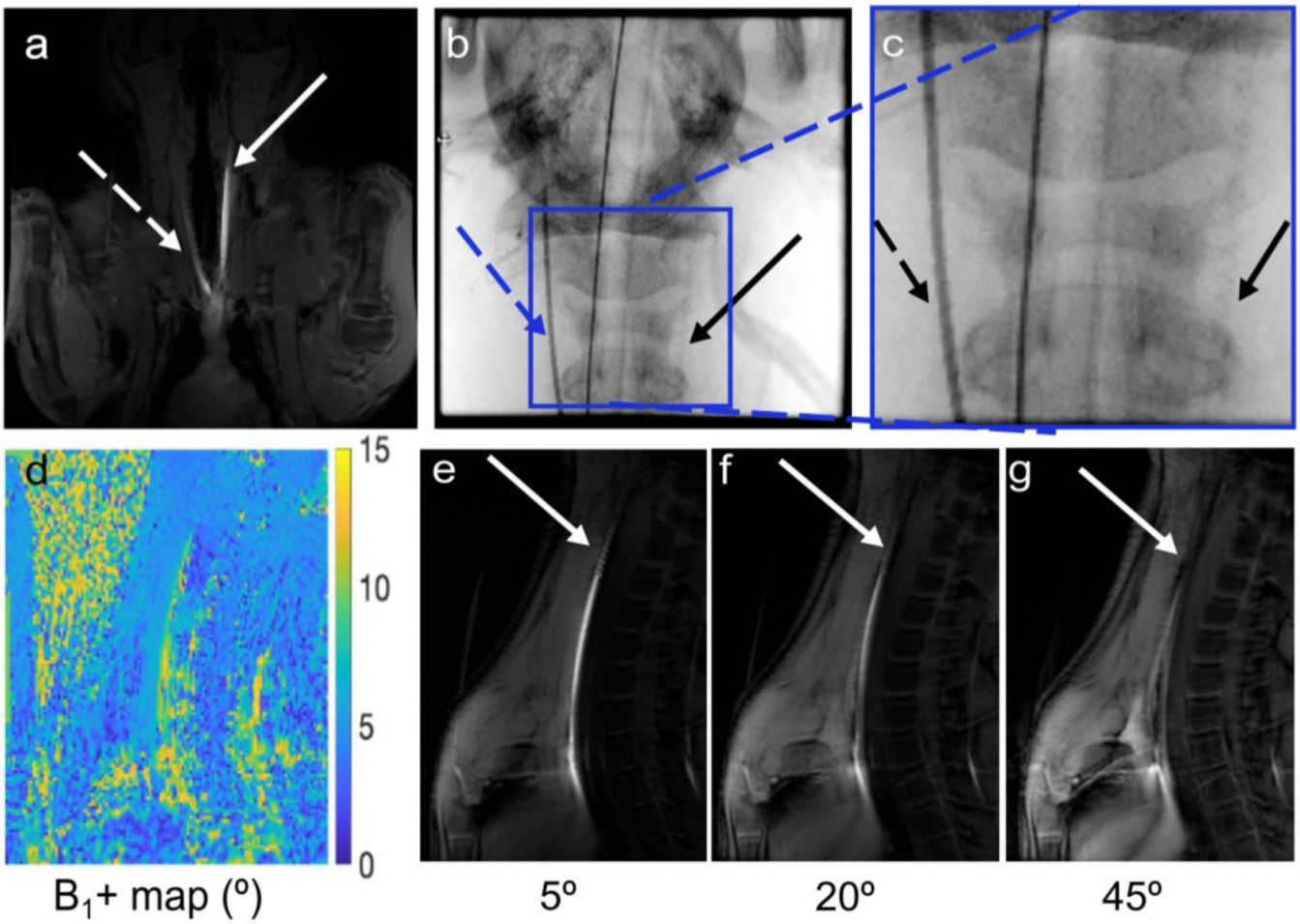

Figure 3.

Wireless resonant marker tracking in vivo at 3.0T. Markers placed in the right (dashed arrow) and left (solid arrow) carotid arteries of a single swine are shown in a coronal scan plane under a) MRI and b) x-ray, which are more easily seen under c) magnification (left artery with contrast, and the right artery without contrast). d) A sagittal B1+ map quantifies signal amplification. Low background signal and high marker signal amplification was demonstrated at a flip angle of e) 5°. Surrounding tissue signal becomes higher and over-flipping near the marker are shown as the flip angle increases to f) 10° and g) 45° [74].

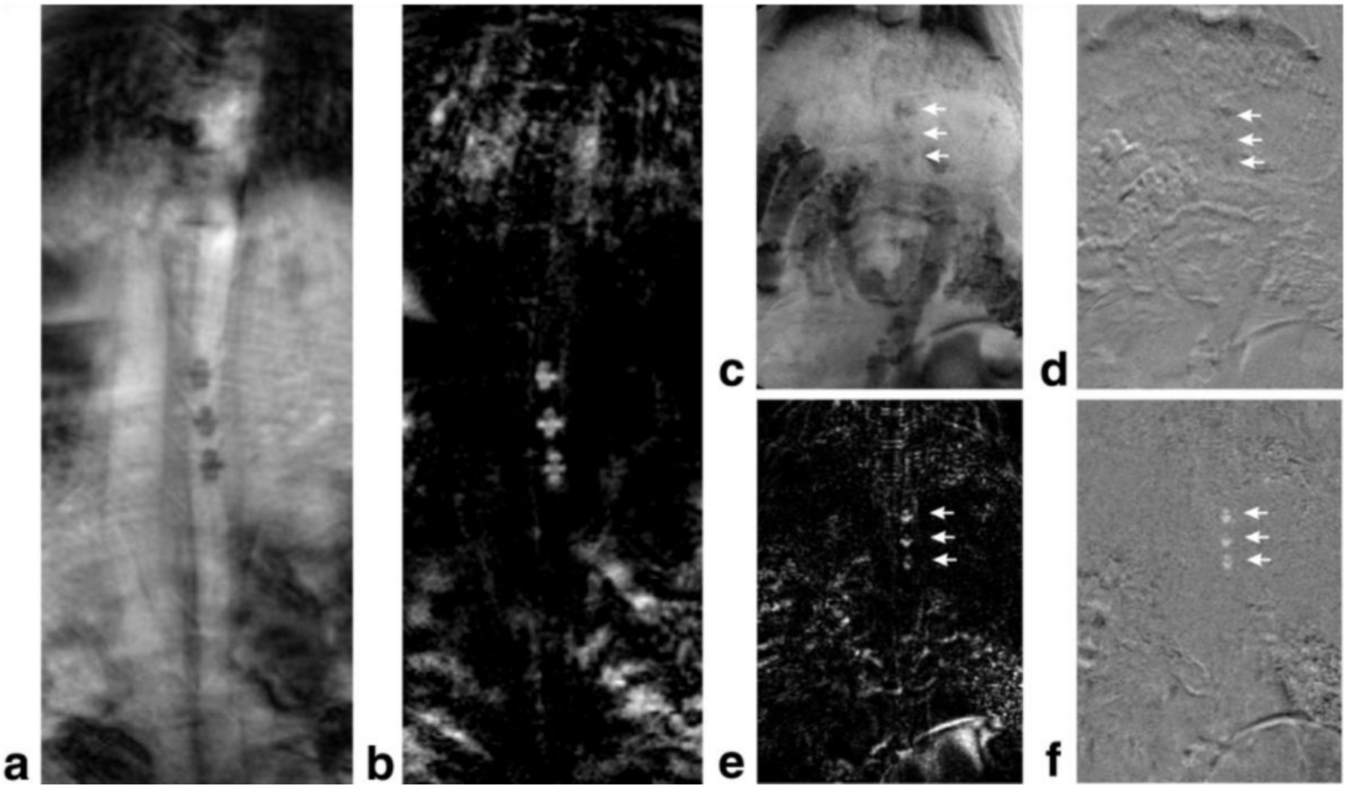

Figure 4.

Passive marker tracking sequences. Visualization of three paramagnetic markers with a) a conventional gradient echo sequence (slice 30 mm, TE/TR = 4.6/60 ms, duration 22 sec) and b) dephased positive contrast gradient echo imaging (white marker sequence with 1.9 cycles of phase across the slice) with similar acquisition parameters. In vivo application of white marker tracking with significant obscuring of the makers for conventional c) unsubtracted and d) subtracted tracking. White marker tracking permits easy detection of the markers for both e) unsubtracted and f) subtracted positive contrast tracking [93].